CHEMISTRY
A EUROPEAN JOURNAL

DOI: 10.1002/chem.200600435

The Tautomeric Forms of Cyameluric Acid Derivatives**

Nadia E. A. El-Gamel,[a] Lena Seyfarth,[b] Jörg Wagler,[a] Helmut Ehrenberg,[c] Marcus Schwarz,[a] Jürgen Senker,[b] and Edwin Kroke*[a]

Abstract: The tautomerism of cyameluric acid $C_6N_7O_3H_3$ (**1a**), cyamelurates and other heptazine derivatives has recently been studied by several theoretical investigations. In this experimental study we prepared stannyl and silyl derivatives of cyameluric acid (**1a**): $C_6N_7O_3[Sn(C_4H_9)_3]_3$ (**3a**), $C_6N_7O_3[Sn(C_2H_5)_3]_3$ (**3b**), and $C_6N_7O_3[Si(CH_3)_3]_3$ (**4**). In order to investigate the structure of **1a** the mono- and dipotassium cyamelurate hydrates $K(C_6N_7O_3H_2)\cdot 2H_2O$ (**5**) and $K_2(C_6N_7O_3H)\cdot 1H_2O$ (**6**) were synthesized by UV/Vis-controlled titration of a potassium cyamelurate solution with aqueous hydrochloric acid. Compounds **3–6** were characterized by FTIR and solid-state NMR spectroscopy as well as simultaneous thermal analysis (TGA, DTA). The single crystal X-ray structures of the salts **5** and **6** show that the hydrogen atoms in both anions are localized on the peripheral nitrogen atoms. This indicates—in combination with the solid-state NMR studies—that the most stable tautomer of solid **1a** is the triketo form with C_{3h} symmetry. However, derivatives of both the hydroxyl and the amido tautomers may be formed depending on the substituent atoms: The spectroscopic data and single crystal structures of compounds $C_6N_7O_3[Si(CH_3)_3]_3$ (**4**) and the solvate $C_6N_7O_3[Sn(C_2H_5)_3]_3\cdot C_2H_4Cl_2$ (**3b′**) show that the former is derived from the symmetric trihydroxy form of **1a**, while **3b′** crystallizes as a chain-like polymer, which contains the tin atoms as multifunctional building blocks, that is, bridging pentacoordinated Et_3SnO_2 and Et_3SnON units as well as non-bridging four-coordinated Et_3SnN units. The cyameluric nucleus is part of the polymeric chains of $C_6N_7O_3[Sn(C_2H_5)_3]_3\cdot C_2H_4Cl_2$ (**3b′**), by the action of both tautomeric forms of cyameluric acid, the amide and the ester form.

Keywords: ^{15}N solid-state NMR spectroscopy · heterocycles · N ligands · potassium · silicon · tin

Introduction

Cyameluric acid **1a** and its salts as well as other derivatives of tri-s-triazine (or s-heptazine[1]) are based on a cyclic system of twelve C–N bonds which surround a central sp^2 hybridized N atom (see Scheme 1). The 14 π-electrons form a doubly cross-conjugated aromatic system.[2] A closely related aromatic system with six π-electrons is the well known and very thoroughly investigated 1,3,5-triazine ring.[3] Examples of both classes of heterocyclic compounds are the title compound **1a** and its analogue cyanuric acid $C_3N_3(OH)_3$ (**2a**) or hydromelonic acid $C_6N_7(NCNH)_3$ (**1b**) which represents the analogue to tricyanomelamine $C_3N_3(NCNH)_3$ (**2b**) (Scheme 1).

We became interested in the class of heptazine compounds because of their potential use as building blocks for

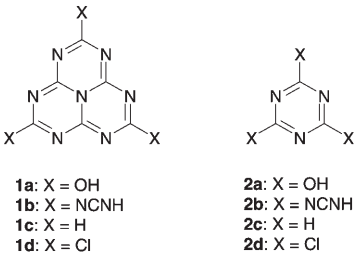

Scheme 1. Selected hepatzine derivatives **1** which are structurally and, with respect to chemical properties, analogous to the 1,3,5-triazine derivatives **2**.

---

[a] Dr. N. E. A. El-Gamel, Dr. J. Wagler, Dr. M. Schwarz,
Prof. Dr. E. Kroke
Institut für Anorganische Chemie, TU Bergakademie Freiberg
Leipziger Strasse 29, 09596 Freiberg (Germany)
Fax: (+49) 3731-39-4058
E-mail: kroke@chemie.tu-freiberg.de

[b] L. Seyfarth, Prof. Dr. J. Senker
Anorganische Chemie I, Universität Bayreuth
95440 Bayreuth (Germany)

[c] Dr. H. Ehrenberg
Leibniz Institut für Festkörper und Materialforschung
Helmholtzstrasse 20
01069 Dresden (Germany)

[**] Tri-s-triazine derivatives, Part 4. For part 3 see ref. [25].

graphitic carbon(IV) nitrides.[4] The latter phases are currently investigated by several research groups, for example, as precursors for diamond-like, sp^3-hybridized carbon(IV) nitrides.[5] Research in this area was initiated through predictions by Cohen who postulated that C_3N_4 materials may exist which might be harder than diamond.[6] Hundreds of experimental studies on attempts to synthesize C_3N_4 as well as related carbon nitride materials were published in the past decade. However, none of them was completely successful, that is, none gave reproducible results on the synthesis of a carbon(IV) nitride.[5]

First derivatives of cyameluric acid have been prepared as early as in the first half of the 19th century.[7] However, they did not attract much attention over the past 150 years and relatively few facts about these compounds are known up to date.[8] The existence of a "cyameluric nucleus" C_6N_7 consisting of three annelated s-triazine rings was first postulated in 1937 by Pauling et al. for **1a** and its derivatives.[9] Attempts to prepare cyameluric esters and amides were reported by Redeman and Lucas in 1940.[10] Cyamelurate salts of the type $(M^{n+})_{3/n}[C_6N_7O_3]$ as well as other s-heptazine derivatives such as the melamin analogue melem $C_6N_7(NH_2)_3$ were investigated in the 1960s and 1970s by Finkel'shtein et al.[11] Based on analyses of the vibrational spectra the studies confirmed the theoretical postulate by Pauling experimentally.

The first comprehensively characterized compound containing the heptazine unit was the parent molecule $C_6N_7H_3$ (**1c**), which was prepared in 1982 by Hosmane, Rossman and Leonard.[12] A set of experiments was performed in order to study the chemical reaction behavior of tri-s-triazine (**1c**). The results were compared with azacycl[3.3.3]azines with less nitrogen atoms. In general, the reactivity decreases and the thermal stability increases within this series of heteroaromatic systems, which are isoelectronic to the phenalene anion.[12a,d]

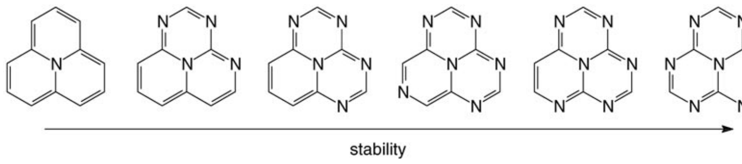

Recent reports were focused on the stability and properties of selected aza-phenalenyl neutral radicals,[13] anions,[14] cations[15] and valence-saturated neutral molecules.[16] In other studies, these nitrogen-based heterocycles were investigated with respect to their relevance for carbon nitrides in general[5,17] and in particular concerning nitrogen-containing graphitic phases,[5,18] fullerenes[19] and CN_x nanotubes.[20]

It took another 20 years after the successful synthesis of the parent $C_6N_7H_3$ molecule until the second crystal structure for a representative of the class of heptazine compounds was reported in 2002,[4] a solvate of the trichloride **1d**. This was followed by a detailed structural investigation of melem $C_6N_7(NH_2)_3$ by Schnick et al. using X-ray diffraction and several spectroscopic techniques,[21] and recently the preparation and structural characterization of a melem adduct and melemium salts.[22] Gillan et al. described the crystal structure of the explosive tri-azide $C_6N_7(N_3)_3$[23] while we investigated some properties and structures of cyamelurates $M_3[C_6N_7O_3]$[24] and melonates $M_3[C_6N_7(NCN)_3]$.[25] Recently, single crystal structures of the solvent free trichloride **1d** and of $C_6N_7(N(C_2H_5)_2)_3$ were described.[26,27] An overview of structural data and properties of heptazine derivatives is presented in Table 1.

In addition to the above described use of heptazine derivatives as precursors for (ultra)hard carbon nitrides, further potential applications include burn-rate suppressants for solid rocket propellants,[28] and flame retardants.[29] The latter proposed application is based on the very high thermal stability of the C_6N_7 nucleus, which decomposes around 500 °C,[24] despite its high nitrogen content. By combination of the heptazine motive with azide- or nitro-substituents, candidates for high energy density materials may be designed.[30] Several authors have described the determination of the surface properties of selected heptazine derivatives and their use as potential stationary phases for ion and gas chromatographic separations.[31,32] Last but not least, the UV absorption, luminescence and NLO properties of heptazine derivatives may be exploited for photo stabilizers (UV protection), sensitizers and emission.[8,24,25,27]

All the compounds mentioned above are exclusively derived from the hydroxyl form of cyameluric acid. In contrast, there are numerous structures of both, cyanuric acid as well as isocyanuric acid derivatives known, which gives an impression of the variability of such tautomeric systems. Therefore, we decided to investigate possible tautomeric forms of **1a** and its derivatives. In this regard, it should be pointed out that several theoretical studies in the past two years were also devoted to heptazine derivatives and in particular focused on the tautomerism of cyameluric acid.[21,30,33–36] Here we present an experimental study on the latter topic.

Results and Discussion

Cyanuric and cyameluric tautomerism: It is well known that derivatives of both, cyanuric acid $C_3N_3(OH)_3$ (**2a**) as well as isocyanuric acid $C_3N_3H_3O_3$ are stable.[37] Among other applications,[3] current interest arises from the utilization of these 1,3,5-triazine derivatives as synthons in supramolecular chemistry.[38] Besides the trihydroxy- and the trioxo forms with C_{3h} symmetry, there are three further less symmetric tautomers of cyanuric acid, as depicted in Scheme 2b. In some cases, cyanuric acid derivatives can be transformed into the symmetric isomer quantitatively simply by heating, such as the reaction given below.[39]

This rearrangement reaction is useful in preparative organic chemistry. It has, for example, been used for the synthesis of important pharmaceutical intermediates.[40]

Table 1. Comparison of structural and spectroscopic properties of s-heptazine derivatives.

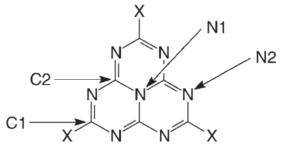

X=	H[a]	Cl[b]	N_3[c]	NH_2[d]	O^-[e]	NCN^-[c,f]
d (N1−C2) [pm]	138.8	139.7	140.0	132–146	140.1	140.5
d (C2−N2) [pm]	133.2	133.4	132.5/ 132.6[c]	131–139	132.5	130.2/ 132.8[c]
d (N2−C1) [pm]	132.6	132.8	134.0/ 133.3[c]	130–140	137.1	136.2/ 136.3[c]
d (C1−X) [pm]	99.5	171.6	140.2	127–136	125.5	134.8
$\sphericalangle$(N2-C1-N2) [°]	128.5	130.2	128.4	126–135	122.9	125.6
$\sphericalangle$(C1-N2-C2) [°]	116.0	115.1	115.5/ 117.0[c]	107–121	118.9	117.3/ 117.9[c]
$\sphericalangle$(N2-C2-N1) [°]	119.7	119.7	118.8/ 120.4[c]	113–127	119.6	120.5/ 118.7[c]
$\sphericalangle$(N2-C2-N2) [°]	120.5	120.6	120.8	113–122	120.8	120.5
$\sphericalangle$(N2-C1-X) [°]	115.6	114.9	113.8/ 117.8[c]	111–117	118.5	113.8/ 120.7[c]
$\sphericalangle$(C2-N1-C2) [°]	120.0	120.0	120.0	117–124	120.0	120.0
m.p. [°C]	> 360	405	(180, decomp)	(560, decomp)	> 450	> 400
^{13}C NMR δ C1/C2 [ppm]	171.6/159.7[g]	175.0/ 158.2[h]	172.2/ 159.2[i]	164.3(166.4)/ 155.1(156.0)[j]	171.3/ 160.9[k]	174.3/ 158.6[l]
IR [cm^{-1}] of C_6N_7 unit	–	1610(vs) 1505(vs) 1310(vs) 825(m)	1606(vs) 1530(vs) 1362(vs) 820(m)	1606(vs) 1469(vs) 1304(vs) 802(m)	1627(s) 1500(vs) 1423(vs) 833(w)	1634(vs) 1500(s) 1440(vs) 801(s)
$\lambda_{max,abs}$ [nm]	443 (ε=268) 305 (22 700)[m]	310	–	288	313	340
$\lambda_{max,em}$ [nm]	517	366	–	466	383	400
lit.	[12a]	[4]	[8,23]	[21]	[24]	[25]

[a] Bond lengths and angles averaged for two independent molecules. [b] Bond lengths and angles averaged for 3.5 independent molecules in [$3.5\times C_6N_7Cl_3\cdot 1$ acetone$\cdot 0.5\,Et_2O$], the solvent free structure of $C_6N_7Cl_3$ is described in [26]. [c] Due to the C_3 symmetry there are two C2-N2-, N2-C1-distances as well as two C1-N2-C2-, N2-C2-N1- and N2-C1-X-angles. [d] Structural data from X-ray powder diffraction, therefore larger variation of the determined values. [e] Values for the lithium salt. [f] Values for the potassium salt. [g] Solvent: [D_6]DMSO, $^1J_{CH}$(C1)=207.6 Hz. [h] Solvent: [D_8]THF. [i] Solvent: [D_6]DMSO. [j] Solid-state NMR data. [k] Solvent: D_2O. [l] Additional signal at 124.9 ppm for C atoms of the cyanamide groups, solvent: D_2O. [m] Solvent: acetonitrile, further maxima and shoulders: 416(ε199), 391 sh(91), 298 sh(18 900), 293(20 600), 279 sh(13 580), 219(9660).

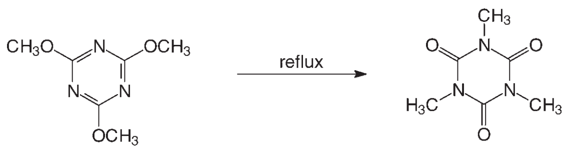

Notably the syntheses and the structures of the above mentioned graphitic carbon(IV) nitrides are also related to the tautomerism of cyanuric acid and its derivatives. Most authors discuss the s-triazine based structures **I** and **II** in Scheme 3, which may be considered as cyanuric acid and cyameluric acid amides, as the most stable forms of C_3N_4.[5] However, reports on the successful syntheses of the alternative graphitic network **III** derived from an asymmetric tautomer of the cyanuric acids have also been published.[41] A similar heptazine based structure **IV** may also be formed.[4,5]

Cyameluric acid has seventeen tautomeric forms: one trihydroxy, three dihydroxy, four tri-oxo and nine monohydroxy isomers (Scheme 2a). It is an open question, which tautomers are stable in the solid-state. In solution equilibria between these forms may be present.

Recently, three theoretical studies were focused on the stability of all these cyameluric acid tautomers relative to each other in the gas phase and in solution.[33c,e,34] Based on DFT calculations the authors came to the conclusion, that the trioxo tautomer **2-5-8** (Scheme 2a) with C_{3h} symmetry is most stable, which is to be expected from simple acidity–basicity considerations for the oxygen atoms and the six peripheral nitrogen atoms of cyameluric acid. The trihydroxy form was calculated to be less stable than the **2-5-8** isomer by more than 80 kJ mol^{-1} in the gas phase. The second most stable tautomer is the trioxo form **2-5-9**, which is about 20 kJ mol^{-1} less stable than **2-5-8**. All other tautomers should be significantly destabilized in the gas phase by more than 45 kJ mol^{-1}.[34] As expected, the proton transfer activation energies are much smaller in methanol and water solution (>50 kJ mol^{-1}) compared with the gas phase (>165 kJ mol^{-1}).[33] The latter results were based on intramolecular proton transfers via four-membered rings in the gas phase, and solvent assisted six-membered ring intermediates in solution. So far, there are no data on intermolecular proton transfers, which might be important for the tautomerism in the solid-state.

Contrary to these theoretical results, cyameluric acid as well as mono- and disubstituted derivatives are usually represented in their hydroxyl forms. One example is the so-called "Mystery Molecule" of Pauling.[42] In this hypothetical compound one of the hydroxyl groups is replaced by an azide unit. Interestingly, the CAS Registry entry for cyameluric acid (Reg.-No.: 1502-46-1) represents the asymmetric tautomer **2-5-9**, which is not very reasonable. The latter is

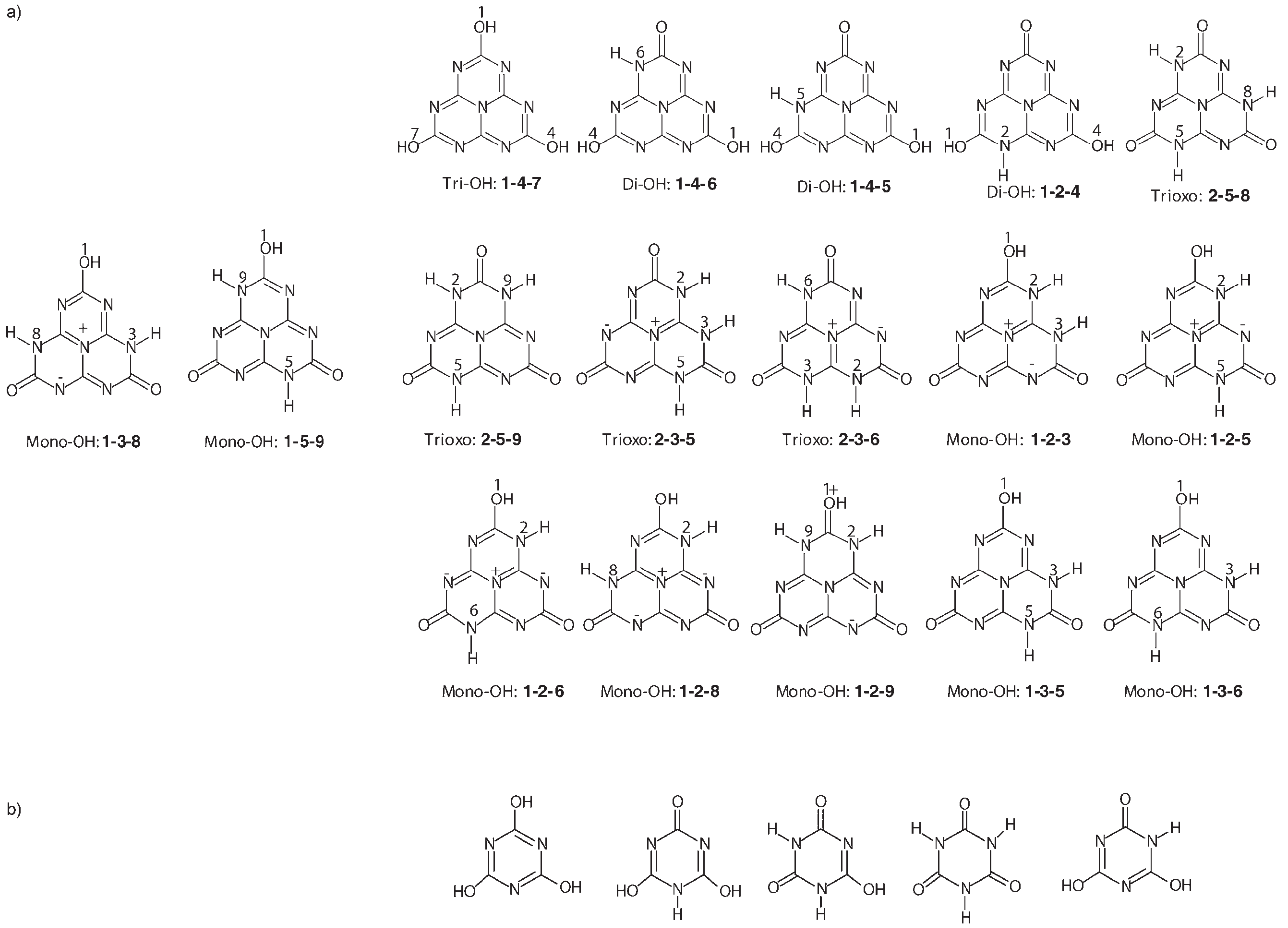

Scheme 2. Tautomeric forms of cyameluric acid (a) and cyanuric acid (b).

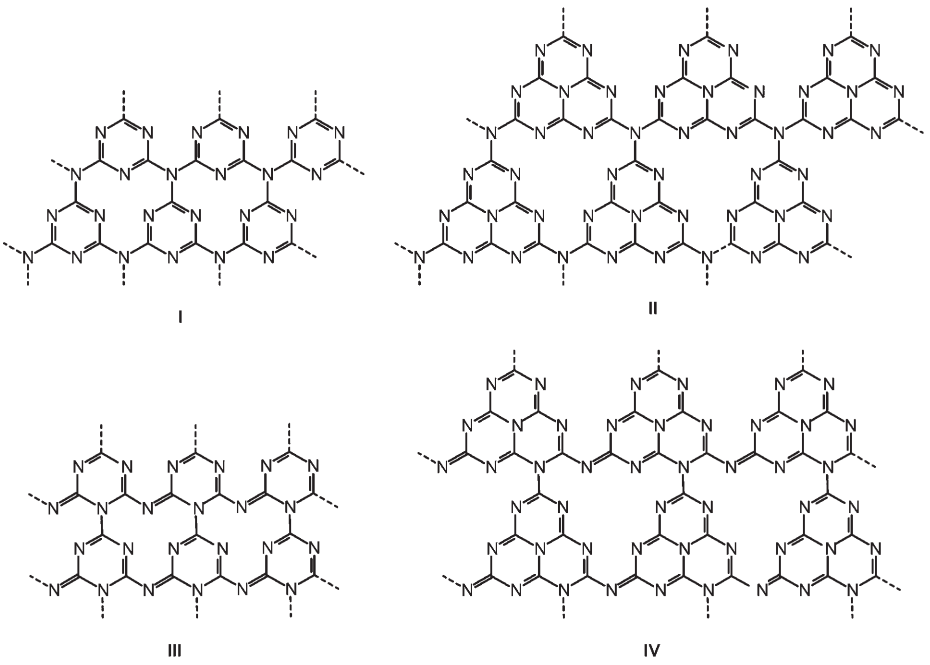

Scheme 3. Four selected graphitic carbon(IV) nitride networks, which have been proposed in the literature. For calculated stabilities and further details on graphitic C_3N_4 see ref. [5].

probably due to the fact, that no differentiation is made in the CAS Registry database between keto–enol tautomers, thus only one entry is found also for cyanuric acid and isocyanuric acid (Reg.-No.:108-80-5).

Synthesis of cyameluric acid derivatives: Cyameluric tri-alkali salts of the type $M_3[C_6N_7O_3]$ are hydrolytically and thermally stable. They can easily be prepared from cyameluric acid with an excess of the corresponding alkali hydroxides in water.[24] The ionization constants of cyameluric acid were determined by Redemann et al. in 1939,[10a] but without any further investigation. Similar acid–base titration experiments with cyameluric acid were described

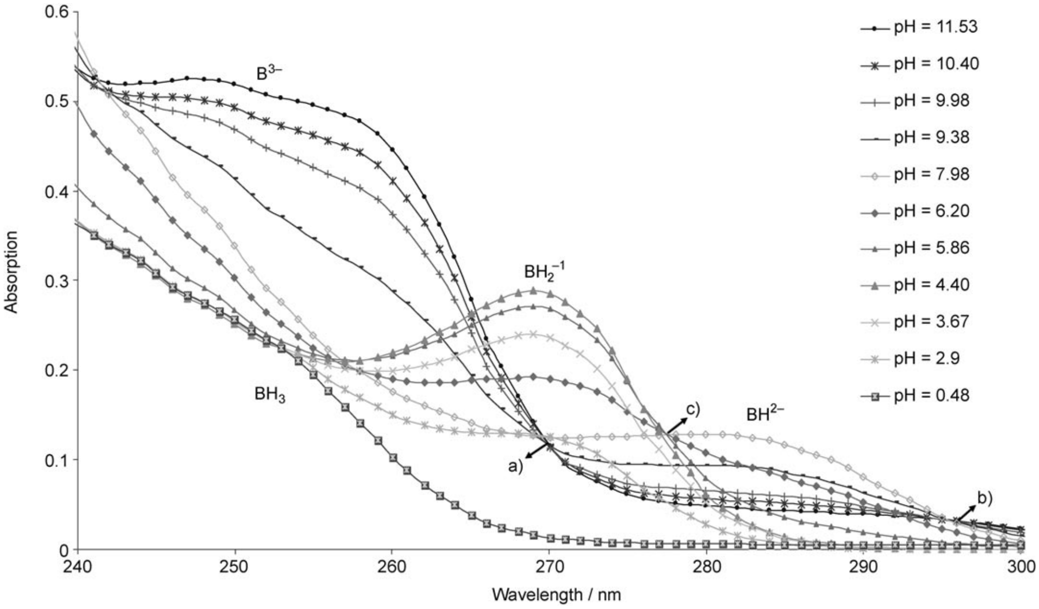

Figure 1. UV absorption spectra of an aqueous solution of potassium cyamelurate titrated with 0.1 M aqueous hydrochloric acid. As expected, a clear step-wise transformation from $[C_6N_7O_3]^{3-}$ ($=B^{3-}$) via the mono- and diprotonated ions $[C_6N_7O_3H]^{2-}$ ($=BH^{2-}$) and $[C_6N_7O_3H_2]^{-}$ ($=BH_2^{-}$) into a solution of non-charged cyameluric acid molecules $C_6N_7O_3H_3$ ($=BH_3$) is observed. Two isosbestic points a) and b) for the reaction from B^{3-} to BH^{2-} can be identified. One further isosbestic point c) corresponds to the transformation of BH^{2-} into BH_2^{-}.

later by two other groups.[43,44] The authors determined the pK_s values (pK_{s1} 3.0–3.1, pK_{s2} 6.1–6.6, pK_{s3} 8.4–9.1), but no structural or spectroscopic data on any monohydrogencyamelurate or dihydrogencyamelurate have been reported. To determine the best pH ranges for the synthesis of pure samples of mono- and dipotassium cyamelurates we also performed a titration experiment, which was monitored by UV/Vis spectroscopy. A diluted solution of $K_3(C_6N_7O_3)$ was titrated with hydrochloric acid, which prevented precipitation of the cyameluric acid. Figure 1 shows a selected set of UV/Vis spectra recorded in the pH range between 11.5 and 0.5. As expected, four different species were detected with decreasing pH and increasing degree of protonation:

$$[C_6N_7O_3]^{3-} \rightarrow [C_6N_7O_3H]^{2-} \rightarrow [C_6N_7O_3H_2]^{-} \rightarrow [C_6N_7O_3H_3]_{aq}$$

The four species show significantly different UV-absorption properties due to their different electronic and molecular structure (see below). The fully deprotonated anion $[C_6N_7O_3]^{3-}$ is characterized by an absorption maximum at ~250 nm ($\varepsilon = 17.2\times10^2\,\mathrm{L\,mol^{-1}\,cm^{-1}}$), with two shoulders around ~270 and ~280 nm (Figure 1). At pH 7.98 the maximum concentration of the monoprotonated anion $[C_6N_7O_3H]^{2-}$ is formed. The spectrum shows a single broad maximum at ~282 nm ($\varepsilon = 4.33\times10^2\,\mathrm{L\,mol^{-1}\,cm^{-1}}$). This transformation from $[C_6N_7O_3]^{3-}$ to $[C_6N_7O_3H]^{2-}$ is characterized by two isosbestic points at 270 and 296 nm (marked a) and b) in Figure 1). A concentration maximum for the doubly protonated anion $[C_6N_7O_3H_2]^{-}$ is indicated at pH 4.40. The spectrum shows a clear absorption peak at ~268 nm ($\varepsilon = 9.73\times10^2\,\mathrm{L\,mol^{-1}\,cm^{-1}}$). An isosbestic point at 278 nm is characteristic for the latter protonation reaction (marked c) in Figure 1). The third transformation into the neutral molecule $[C_6N_7O_3H_3]_{aq}$ causes a disappearance of any absorption above $\lambda = 275$ nm and a featureless spectrum with a continuous absorption increase from 270 to 240 nm. Therefore, no characteristic isosbestic point can be identified for the transformation from $[C_6N_7O_3H_2]^{-}$ into $[C_6N_7O_3H_3]_{aq}$. The described changes in the UV spectra are due to a protonation of the cyameluric nucleus at the peripheric nitrogen atoms (see below). The absorption bands can be attributed to π–π* and/or n–π* transitions inside the heptazine molecule.

For the preparation of pure and crystalline samples of mono- and dipotassium cyamelurates $K(C_6N_7O_3H_2)$ and $K_2(C_6N_7O_3H)$ more concentrated solutions of potassium cyamelurate $K_3(C_6N_7O_3)$ were again titrated with HCl until the corresponding pH values were reached. Crystallization was initiated by slow diffusion of ethanol vapor into the filtered solution of the respective salt.

In addition to the two salts we wanted to prepare neutral molecular derivatives of different tautomeric forms of cyameluric acid. The syntheses of tris(tri-*n*-butylstannyl)-cyamelurate (**3a**) and tris(triethylstannyl)-cyamelurate (**3b**) were accomplished by stannylation with hexa-*n*-butyl- and hexaethyldistannoxane, respectively.[45] An analogous route was described for tris(triethylgermyl)-cyamelurate.[46] In summary, compounds **3**–**6** were prepared according to Scheme 4. Further details are provided in the Experimental Section.

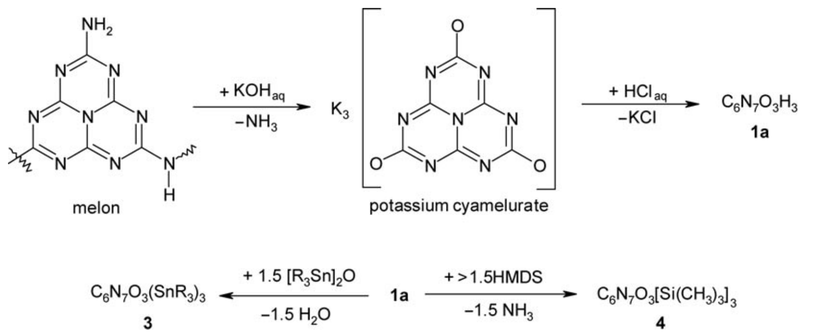

Scheme 4. Synthesis of potassium cyamelurate $K_3[C_6N_7O_3]$, cyameluric acid $C_6N_7O_3H_3$ (**1a**), $C_6N_7O_3[SnR_3]_3$ (**3a** R = *n*Bu; **3b** R = Et) and $C_6N_7O_3[Si(CH_3)_3]_3$ (**4**).

Vibrational spectroscopy: FTIR spectra of the mono- and dipotassium salts **5** and **6** are represented in Figure 2a and b. The spectra are similar and agree well with the data reported for the tri-alkali salts.[24] In particular, absorption bands corresponding to the cyameluric nucleus appear at 1680(vs), 1540(vs), 1450(s), 1400(vs) and 800(m) cm^{-1}, respectively. Furthermore, a very broad band around 2400–3400 cm^{-1} corresponding to OH stretching modes is due to the incorporation of water in the salts. The N–H valence vibration is most likely responsible for the absorption bands around 3500 cm^{-1}. Several further signals in the finger print region of the spectra are less straightforward to be assigned.

The FTIR spectra of **4** (Figure 2c) and **3a** (Figure 2d) differ significantly from the spectra of the salts. This is in part due to the lack of N-H and O-H groups as well as the absence of crystal water in these compounds. Compound **4** (Figure 2c) is characterized by the presence of absorption bands at 1658(vs), 1451(vs) and 812(m) cm^{-1} for the heptazine unit, and a sharp band at 1011(s) cm^{-1} for Si-O-C units. The Si-CH_3 motif is indicated by two characteristic bands at 1265(vs) and 844(s) cm^{-1}, besides there are two bands at 2963(m) and 2845(s) cm^{-1} for symmetric and asymmetric CH_3 stretching vibrations, respectively.

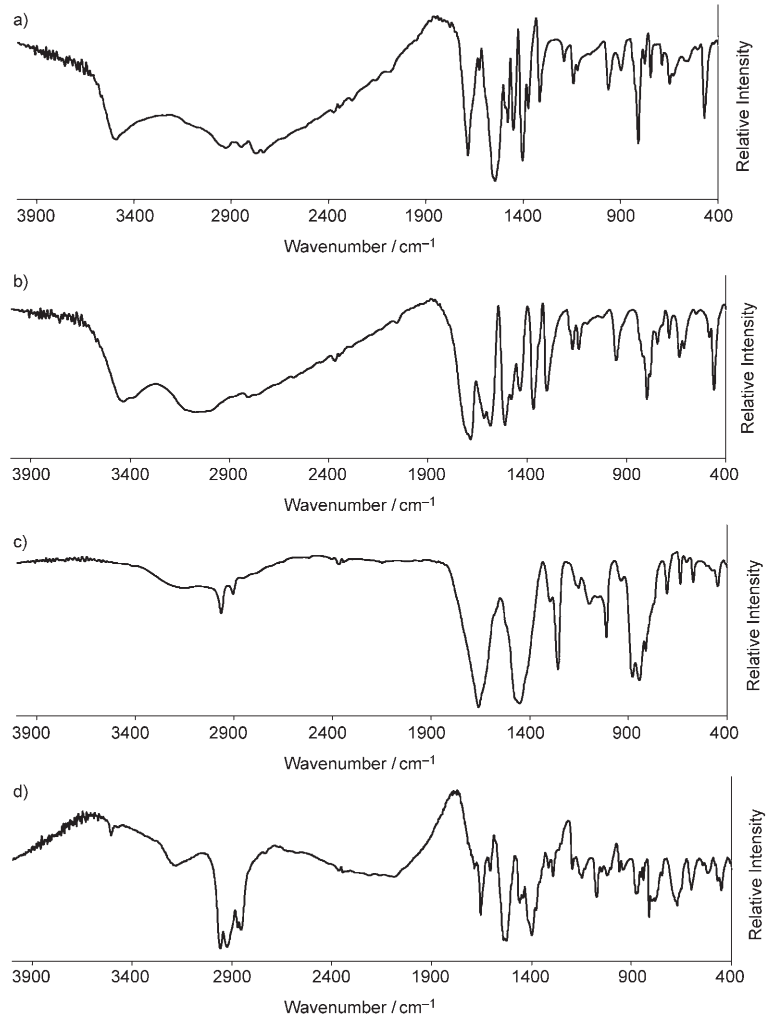

Figure 2. FTIR spectra of potassium cyamelurates a) $K_2(C_6N_7O_3H)\cdot 1H_2O$ (**6**) and b) $K(C_6N_7O_3H_2)\cdot 2H_2O$ (**5**); of the molecular derivates c) $C_6N_7O_3[Si(CH_3)_3]_3$ (**4**) and d) $C_6N_7O_3[Sn(C_4H_9)_3]_3$ (**3a**).

The FTIR spectrum of tris(tri-*n*-butylstannyl)cyamelurate (Figure 2d) is characterized by a shift in the absorption bands of the heptazine ring system to 1526(vs), 1398(vs) and 876(m) cm^{-1} and a band at 1645(st) cm^{-1}, which may be due to a $C{=}O$ band. There is an additional band at 811(m) cm^{-1}. The *n*-butyl groups cause several strong absorption bands in the range of 2923 to 2853(vs) cm^{-1}.

Solid-state NMR spectroscopy: ^1H, ^{13}C and ^{15}N MAS NMR spectra were recorded for the compounds **3b**, **4**, **5** and **6** (Figures 3–5). A detailed assignment of the observed resonances is given in Tables 2–4. The spectral analysis allowed us to corroborate the results of the diffraction experiments and to provide suitable reference data for a detailed examination of cyameluric acid, which will be presented in a forthcoming publication.

The ^{1}H spectra of **3b**, **4**–**6** (Figure 3) reveal three characteristic hydrogen bearing molecular fragments. The trimethylsilyl and triethylstannyl groups of the compounds **3b** and **4** lead to broad resonances in the range δ 0–2 ppm (Table 2). The signals for the tricyclic anions (**5**, **6**) at δ 12.8 ppm ($[C_6N_7O_3H]^{2-}$) and at 11.1 ppm and 14.2 ppm ($[C_6N_7O_3H_2]^{-}$) support the existence C_2N-H groups for both compounds. The signals at 4.3/4.7 ppm and 6.9 ppm are typical for H_2O molecules embedded in a hydrogen-bonding network.[47–49] The splitting of the resonances for compound **5** demonstrates the existence of hydrogen bonds, which differ significantly in their strength. This as well as the intensity ratio of these signals at δ 14.2 and 11.1 ppm of 1:3 corresponds very well to the crystal structure (see below), where one short hydrogen bond (1.84 Å for O7···H14) and three relatively long hydrogen bonds (2×1.93 und 1×1.97 Å) are observed. Furthermore the intensity ratio I(OH):I(NH) was determined to 2:1 for both compounds which is in excellent agreement with the structure models derived from the diffraction data (see below).

In the ^{13}C NMR spectra (Figure 4) the aliphatic groups of the compounds **3b** and **4** cause several strong signals between δ 0 and 20 ppm (Table 3). In the aromatic region the resonances of all four compounds are arranged in two groups. In accordance to the literature the downfield shifted signals can be assigned to OCN_2 fragments. Compound **3b** exhibits the largest chemical shift value (169.5 ppm) whereas **5** reveals the smallest shift (164.0 ppm). Similar values of XCN_2 groups are reported for $C_6N_7H_3$ (171.6 ppm),[12] $C_6N_7Cl_3$ (175.0 ppm),[4] $C_6N_7(NH_2)_3$ (164.3 ppm, 166.4 ppm)[21] and $[C_6N_7O_3]^{3-}$ (171.3 ppm).[24] The averaged shift $\delta(OCN_2)$ of the tricyclic anions $[C_6N_7O_3H_x]^{(3-x)-}$ as a function of the protonation degree ($x = 0$, 1, 2) shares a linear trend. By reducing the charge of the anions about one unit an upfield shift of 3.5 ppm occurs.

The second group of resonances (150–160 ppm) consists of either CN_3 or OCN(NH) fragments (Figure 4). In the case of **3b** and **4** the assignment is straight forward. The signals at 152.9 ppm and 156.3 ppm (**3b**) as well as the resonance at 158.9 ppm can unambiguously be attributed to CN_3 fragments. Similar shifts are found in the literature for $C_6N_7H_3$ (159.7 ppm),[12] $C_6N_7Cl_3$ (158.2 ppm),[4] $C_6N_7(NH_2)_3$ (155.1 ppm, 156.0 ppm)[21] and $[C_6N_7O_3]^{3-}$ (160.9 ppm).[24] For the mono- and diprotonated heptazine rings, an assignment is difficult due to the overlap of resonances arising from OCN(NH) and CN_3 fragments. Making use of the trend derived above ($\Delta\delta/e = -3.5$ ppm/e) the CN_3 fragments can probably be attributed to the downfield shifted signals 154.1 (**5**) and 158.5 ppm (**6**). Consequently the resonances at 151.8 (**5**) and 154.2 ppm (**6**) belong to the OCN(NH) fragments.

Due to the large variation of the chemical shift and the limited data in the literature the assignment of the ^{15}N spectra is more complex. Up to now only for $C_6N_7H_3$[12] and

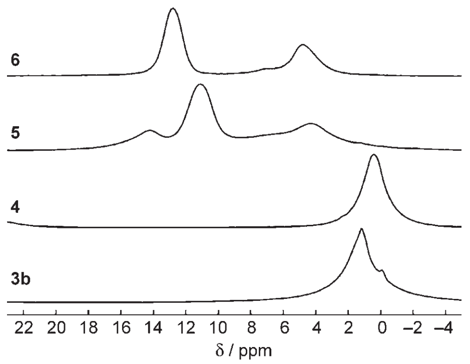

Figure 3. ^{1}H MAS NMR spectra for the compounds $C_6N_7O_3[Sn(C_2H_5)_3]_3$ (**3b**), $C_6N_7O_3[Si(CH_3)_3]_3$ (**4**), $K(C_6N_7O_3H_2)\cdot 2H_2O$ (**5**) and $K_2(C_6N_7O_3H)\cdot 1H_2O$ (**6**).

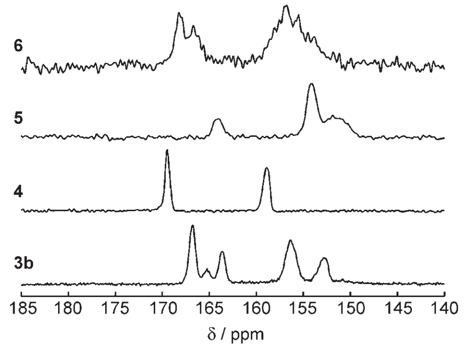

Figure 4. ^{13}C MAS NMR spectra for the compounds $C_6N_7O_3[Sn(C_2H_5)_3]_3$ (**3b**), $C_6N_7O_3[Si(CH_3)_3]_3$ (**4**), $K(C_6N_7O_3H_2)\cdot 2H_2O$ (**5**) and $K_2(C_6N_7O_3H)\cdot 1H_2O$ (**6**). Only the region of the aromatic carbon atoms is displayed. Resonances in the aliphatic region are given in Table 3.

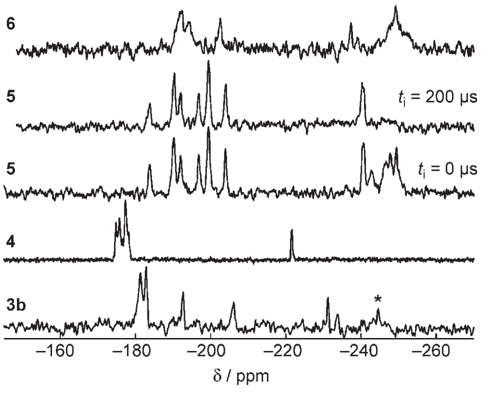

Figure 5. ^{15}N MAS NMR spectra for the compounds $C_6N_7O_3[Sn(C_2H_5)_3]_3$ (**3b**), $C_6N_7O_3[Si(CH_3)_3]_3$ (**4**), $K(C_6N_7O_3H_2)\cdot 2H_2O$ (**5**) and $K_2(C_6N_7O_3H)\cdot 1H_2O$ (**6**). In the spectrum of **3b** the resonance at −245.5 ppm arises from a small impurity due to partial hydrolysis during the experiment and is therefore marked with an asterisk. The two spectra for compound **5** were measured using a CPPI sequence. A polarization inversion time $t_i = 0$ μs reflects a normal CP MAS experiment. For t_i around 200 μs the resonance intensity originating from NH groups diminishes to zero, NH_2 groups exhibit inversed polarization, whereas signals from tertiary nitrogen atoms remain nearly unaffected.[21,22]

Table 2. Assignment of the ^1H MAS NMR spectra for the compounds **3b** and **4–6**.

δ [ppm]	C_2N-H	H_2O	Alkyl
6	12.8(s)	4.7(m), 6.9(vw)	–
5	11.1(s), 14.2(m)	4.3(m), 6.9(w)	–
4	–	–	0.5
3b	–	–	0.1, 0.9, 1.3, 1.6

Table 3. Assignment of the ^{13}C MAS NMR spectra for the compounds **3b**, **4–6**.

δ [ppm]	OCN_2	OCN(NH)	CN_3	Alkyl
6	166.6(m), 168.2(m)	154–159	–	
5	164.0(m)	151.8(s)	154.1(s)	–
4	169.5(m)	–	158.9(m)	0.9(s), 1.4(vs)
3b	163.6(m), 165.2(w), 166.8(s)	–	152.9(m), 156.3(s)	7.3(vw), 8.6(w), 10.1(s), 10.8(s), 11.3(s), 12.0(s), 12.4(m), 16.1(w), 17.4(m), 18.0(m), 20.2(m)

$C_6N_7(NH_2)_3$[21,22] ^{15}N NMR data are available. For $C_6N_7H_3$ the ring nitrogen atoms were observed at −141.4 ppm and the central nitrogen atom was found at −193.4 ppm. Melem shows resonances between δ −197.1 and −205.3 (NC_2), at −234.2 ppm (NC_3) and between −267.1 and −281.6 ppm (NH_2). Obviously, substitution of a terminal group in a tri-s-triazine system causes a change of the chemical shift up to 60 ppm.

Nevertheless the ^{15}N NMR resonances for **4** can unambiguously be assigned based on the pattern splitting. Since the asymmetric unit consists of only one molecule (see below), the group of five resonances (−178.1 to −174.8 ppm) has to be attributed to the six nitrogen atoms in the outer ring whereas the single resonance at −221.5 ppm belongs to the central nitrogen (Figure 5). In the case of compound **3b** two independent molecules occupy the asymmetric unit. The molecules form a chain-like polymer with the $SnEt_3$ groups functioning as connectors as well as terminal groups (see discussion on the crystal structure). The appearance of only few resonances arranged in doublets in the ^{15}N spectrum indicates that both molecules in the asymmetric unit are similar or a crystal lattice type bearing only one independent molecule of **3b** is present in the solvent free form. Based on these considerations and the assignment accomplished for compound **3b** the signals −182.8/−181.3 ppm and −233.9/−231.2 ppm can attributed to NC_2 and NC_3 fragments, respectively. Consequently, the resonances at δ −192.6 and −206.1 ppm belong to C_2N–$SnEt_3$ units.

For the assignment of the tricyclic anions it was necessary to additionally measure a CPPI filtered spectrum for **5** (second spectrum from top of Figure 5). The inversion time t_i was adjusted to eliminate resonances from C_2N-H groups. By comparison with the CP MAS spectra it becomes obvious that the resonances δ −249.3, −247.7, −246.6 and −242.7 (**5**) as well as −249.1 ppm (**6**) originate from C_2N-H fragments. All other signals belong to tertiary nitrogen atoms. Based on the grouping of the resonances furthermore the signals at −240.6 (**5**) and −237.2 ppm (**6**) reveal the central nitrogen (C_3N) whereas all other signals belong to nitrogen atoms in the outer ring.

Table 4. Assignment of the ^{15}N MAS NMR spectra for the compounds **3b** and **4–6**. The asterisk marks a small impurity due to hydrolysis of the sample during the measurement.

δ [ppm]	C_2N	NC_3	C_2N-X	
			X=H	X=$SnEt_3$
6	−202.5(w), −194.1(w), −192.5(m), −190.7(w)	−237.3(w)	−252.3(w), −249.2(m)	–
5	−203.9(m), −199.5(s), −196.8(m), −192.1(m), −190.2(s), −183.8(m)	−240.6(m)	−249.3(m), −247.7(m), −246.6(m), −242.7(w)	–
4	−178.1(m), −177.3(s), −176.6(m), −175.7(m), −174.8(m)	−221.5(m)	–	–
3b	−182.8(m), −181.3(m)	−233,9(w), −231.2(w)	−244.5(vw)*	−206.1(w), −192.6(w)

Crystal structures of 5 and 6: In order to provide clear evidence which of the $[C_6N_7O_3H_{3-x}]^{x-}$ isomers is most stable in the solid-state, we determined single crystal X-ray structures of the hydrates $K(C_6N_7O_3H_2)\cdot 2H_2O$ (**5**) and $K_2(C_6N_7O_3H)\cdot 1H_2O$ (**6**). Selected crystal parameters and refinement data are summarized in Table 5. Interatomic distances and bond angles are shown in Table 6.

The tricyclic anions $[HC_6N_7O_3]^{2-}$ and $[H_2C_6N_7O_3]^-$ of both salts are planar, since the sum of the bond angles around each atom are 360(±0.2)°. This can be attributed to a sp^2 hybridization of all nitrogen and carbon atoms of the conjugated π electron system, that is, of the C_6N_7 heptazine units. The same was found for potassium melonate $K_3[C_6N_7(NCN)_3]$,[25] alkali cyamelurates $M_3[C_6N_7O_3]$,[24] the mono- and diprotonated cationic melemium species in $[HC_6N_7(NH_2)_3]ClO_4$ and $[H_2C_6N_7(NH_2)_3]SO_4$,[22] as well as for non-ionic heptazine derivatives, such as melem $C_6N_7(NH_2)_3$,[21] triazido-tri-s-triazine $C_6N_7(N_3)_3$,[8,23] or trichloro-tri-s-triazine $C_6N_7Cl_3$.[4,26]

It was possible to locate the hydrogen atoms for both the mono- as well as the diprotonated cyamelurate anions. As it was expected, N−H bonds are formed in both cases (Figure 6). The two anions of the asymmetric unit of the mono-potassium salt $K[C_6N_7O_3H_2]\cdot 2H_2O$ (Figure 6a) are protonated at N2 and N4 as well as on N12 and N14, which can be expected if the anion is derived from the cyameluric acid tautomer **2-5-8** (compare Scheme 2). The analogous protonation pattern was observed for the cation $[H_2C_6N_7(NH_2)_3]^{2+}$ in the sulfuric acid of melem.[22]

Only very small distortions of the perfect threefold symmetry as observed for the heptazine derivatives listed in Table 1 can be found for the cyamelurate anions in compound **5** and **6**. A slight elongation of the N−C(O) bond length of the protonated N atoms (1.39–1.40 Å) is found compared with the analogous N−C(O) bond of the non-protonated peripheral N atoms (1.35–1.38 Å). The latter value

Table 5. Selected crystal parameters and refinement data for compounds **3b′**, **4**–**6**.

	5	**6**	**4**	**3b′**
formula	$C_{12}H_{12}K_2N_{14}O_{10}$	$C_6H_3K_2N_7O_4$	$C_{15}H_{27}N_7O_3Si_3$	$C_{52}H_{98}Cl_4N_{14}O_6Sn_6$
M [g mol^{-1}]	590.56	315.35	437.71	1869.38
crystal system	monoclinic	monoclinic	trigonal	triclinic
space group	$P2_1/c$ (no. 14)	$P2_1/n$ (no. 14)	$P31c$ (no. 159)	$P\bar{1}$ (no. 2)
cell parameters				
a [Å]	9.1784(6)	7.4048(5)	25.3601(5)	12.3097(4)
b [Å]	34.681(2)	15.5081(9)	25.3601(5)	14.6623(4)
c [Å]	6.4578(4)	9.5745(6)	7.0299(2)	20.7619(7)
α [°]	90.00	90.00	90.00	94.962(1)
β [°]	92.190(2)	109.259(7)	90.00	101.635(2)
γ [°]	90.00	90.00	120.00	105.281(1)
V [Å^3]	2054.1(2)	1037.95(7)	3915.45(16)	3501.64(19)
Z	4	4	6	2
ρ_{calcd} [g cm^{-3}]	1.910	2.018	1.114	1.773
T [K]	296(2)	293(2)	223(2)	90(2)
λ [Å]	0.71073	0.71073	0.71073	0.71073
cryst. size [mm]	$0.22 \times 0.14 \times 0.01$	$0.30 \times 0.26 \times 0.25$	$0.4 \times 0.2 \times 0.12$	$0.53 \times 0.24 \times 0.18$
μ [mm^{-1}]	0.554	0.940	0.207	2.313
Θ_{max} [°]	28.0	26.4	29.0	38.5
index range	$-12 \leq h \leq 12$ $-45 \leq k \leq 45$ $-8 \leq l \leq 8$	$-9 \leq h \leq 8$ $-19 \leq k \leq 19$ $-11 \leq l \leq 11$	$-34 \leq h \leq 32$ $-34 \leq k \leq 34$ $-9 \leq l \leq 9$	$-21 \leq h \leq 21$ $-25 \leq k \leq 25$ $-36 \leq l \leq 36$
param./restrain.	379/34[a]	184/0	253/1	811/36
total no. reflns	14839	5860	47062	175398
unique reflns	4942	2064	6941	39362
obsd reflns (R_{int})	3141 (0.0294)	1883 (0.0265)	5737 (0.0292)	30320 (0.0339)
absorpt. corr.	multi-scan	none	multi-scan	multi-scan
GoF on F^2	0.989	1.111	1.095	1.116
$R[I>2\sigma(I)]$				
$R1$	0.0372	0.0350	0.0423	0.0395
$wR2$	0.0920	0.0963	0.1127	0.0855
R_{all}				
$R1$	0.0732	0.0389	0.0550	0.0649
$wR2$	0.1018	0.0992	0.1181	0.0946
min/max electron density [Å^{-3}]	−0.261/0.375	−0.262/0.389	−0.251/0.472	−1.847/3.312

[a] All N–H and O–H bond lengths fixed.

was also reported for $[C_6N_7O_3]^{3-}$ ions (1.37 Å). This distortion may be expected from simple consideration of the possible mesomeric Lewis structures with negative charges only on the oxygen atoms, since there are exclusively C–N single bonds to the N-H group.

The C–O bond lengths within cyamelurate anions vary little. Values of 1.21–1.23 Å are found for the twofold protonated cyamelurate, 1.23–1.26 Å for the singly protonated anion and 1.25–1.30 Å for the non-protonated ions in the alkali cyamelurates were determined. The slight increase may be due to the increasing negative charge from −1 to −3, which is in part located on the oxygen atoms. The C–N bond lengths to the central nitrogen atoms of 1.37–1.41 Å are almost identical to the values found for all other heptazine derivatives which have been structurally characterized so far (see Table 1). Nevertheless, all C–N bonds in **5** and **6** are significantly shorter than the normal C–N single bond length (1.470 Å) and longer than the normal C=N double bond (1.280 Å), which is obviously due to the conjugation over the whole heptazine unit.

With respect to bond angles, the protonation on the N atoms is accompanied with a slight increase of the C-N-C bond angles from 117–120° for all non-protonated peripheral nitrogen atoms in $[C_6N_7O_3H_{3-x}]^{x-}$ ions to about 123–125°. The average N-C(O)-N angle is ≅ 120° in both potassium salts, which is smaller than the average bond angle in alkali-cyamelurates (123–125°). Besides, it is smaller than the average N-C(Cl)-N angle (130.2°) in tri-chloro-tri-s-triazine and the N-C(H)-N angle (128.5°) in tri-s-triazine.

Both, the mono- and dipotassium cyamelurates **5** and **6** crystallize as hydrates containing two or one equivalents of crystal water per $[C_6N_7O_3H_{3-x}]^{x-}$ anion, respectively. More crystal water molecules were found in the alkali cyamelurates $M_3[C_6N_7O_3]\cdot xH_2O$ with M = Li, Na, K and Rb, for which x was reported to be from three up to six.[24] The lone pair electrons of two of the four H_2O molecules in the asymmetric unit of $K(C_6N_7O_3H_2)\cdot 2H_2O$ (**5**) form hydrogen bonds to the protons on the cyamelurate anions, indicated by distances of 1.83 Å for N14H···O7 and 1.89 Å for N2H···O9. The latter water molecules are at the same time coordinated (by the other oxygen lone pair) to K2 with d(K2–O9) = 3.07 Å (Figure 6a). A significantly longer distance of 3.35 Å is present between K2 and O7, although this water molecule still may be considered to be part of the first coordination sphere of K2. The other two water molecules of the asymmetric unit of **5** are coordinated to the potassium cations with distances of 2.86 Å for O8–K2 and 2.81 Å for O10–K1. At the same time these water molecules form hydrogen bridges to two N atoms of two different cyamelurate ions with OH···N distances of 2.11–2.16 Å. Hydrogen bridges are also present between the coplanar cyamelurate anions forming layers. These hydrogen bond distances are d(N12H···O2) = 1.94 and d(N4H···O4) = 1.96 Å.

A different hydrogen bonding and metal coordination pattern is present in the asymmetric unit of $K_2(C_6N_7O_3H)\cdot 1H_2O$ (**6**). Bridges between K1 and K2 are formed by the oxygen atom of one water molecule with almost identical K–O distances of 2.78 Å to K1 and K2. One proton of this water molecule forms a hydrogen bridge of d(OH···O2) = 1.94 Å to an oxygen atom of the $[C_6N_7O_3H]^{2-}$ ion. The water molecule is in the same plane as the coplanar anions, which are interconnected by N-H···O hydrogen bridges of 2.03 Å.

Table 6. Selected interatomic distances and bond angles for the potassium cyamelurate **5** (compare Figure 6a).

Bond length [Å]		Bond angle [°]	
O1−C1	1.216(2)	O1-C1-N3	122.04(17)
C1−N2	1.387(2)	O1-C1-N2	120.18(16)
N2−H2	0.849(12)	N2-C1-N3	117.78(15)
N2−C6	1.347(2)	C1-N2-C6	124.90(15)
C1−N3	1.377(2)	C1-N2-H2	118.2(14)
N3−C2	1.299(2)	C6-N2-H2	116.9(14)
C2−N1	1.380(2)	N2-C6-N1	114.74(16)
C6−N1	1.387(2)	N2-C6-N7	122.30(15)
C4−N1	1.418(2)	N1-C6-N7	122.95(15)
C2−N4	1.344(2)	C1-N3-C2	118.23(16)
N4−C3	1.402(2)	N3-C2-N1	124.07(15)
C3−N5	1.361(2)	N3-C2-N4	120.84(17)
N5−C4	1.329(2)	N1-C2-N4	115.09(15)
C4−N6	1.310(2)	C2-N4-H4	119.8(14)
N6−C5	1.368(2)	C3-N4-H4	115.7(14)
C5−N7	1.396(2)	C2-N4-C3	124.37(16)
N4−H4	0.848(12)	C2-N1-C6	120.02(14)
C3−O3	1.218(2)	C2-N1-C4	122.10(14)
C5−O2	1.231(2)	C4-N1-C6	117.87(15)
K1−O2	3.0695(15)	C6-N7-C5	117.54(15)
K1−N6	3.0227(15)	N1-C4-N5	119.35(16)
K1−O6	2.8363(14)	N1-C4-N6	119.73(15)
K1−O10	2.8402(17)	N5-C4-N6	120.92(15)
K2−O3	2.7648(13)	C3-N5-C4	120.81(15)
K2−O8	2.8707(15)	C4-N6-C5	119.67(15)
K2−O9	3.088(2)	N6-C5-N7	122.01(16)
K2−N9	3.1256(15)	N6-C5-O2	119.57(16)
K2−O4	3.1119(14)	O2-C5-N7	118.41(16)

Table 7. Selected interatomic distances and bond angles for the potassium cyamelurate **6** (compare Figure 6b).

Bond length [Å]		Bond angle [°]	
O1−C2	1.247(2)	N7-C1-N1	119.62(14)
C2−N2	1.372(2)	N2-C1-N1	119.60(14)
C2−N3	1.381(2)	N2-C1-N7	120.78(14)
N2−C1	1.322(2)	C2-N2-C1	118.82(14)
N3−C3	1.315(2)	N2-C2-N3	123.10(14)
N4−C3	1.332(2)	O1-C2-N3	118.26(15)
C3−N1	1.4097(19)	O1-C2-N2	118.63(16)
N1−C1	1.4044(19)	C2-N3-C3	118.58(14)
C1−N7	1.326(2)	N3-C3-N1	119.91(14)
C4−N4	1.348(2)	N3-C3-N4	120.06(14)
C4−N5	1.390(2)	N1-C3-N4	120.02(14)
C4−O2	1.2392(19)	C3-N4-C4	119.70(14)
N5−C5	1.351(2)	C3-N1-C5	121.81(13)
C5−N1	1.3782(19)	C3-N1-C1	119.85(13)
C5−N6	1.306(2)	C5-N1-C1	118.33(13)
C6−N7	1.363(2)	C1-N7-C6	119.10(14)
C6−N6	1.389(2)	N4-C4-O2	122.61(16)
C6−O3	1.248(2)	N4-C4-N5	119.79(14)
K1−O3	2.7537(15)	O2-C4-N5	117.60(15)
K1−O1	2.6479(14)	C4-N5-C5	123.34(14)
K1−O2	2.6790(14)	C5-N6-C6	116.54(14)
K1−O4	2.7740(18)	K1-N6-K2	77.92(3)
K1−N4	2.8855(15)	C5-N6-K2	104.27(10)
K2−N6	3.0568(15)	C6-N6-K1	115.41(10)
K−N6	3.2509(15)	N7-C6-N6	122.96(14)

Both salts **5** and **6** may be considered as layered structures (Figure 7). As mentioned above the disc-shaped anions are arranged coplanar forming π-stacked, graphite-like sheets.

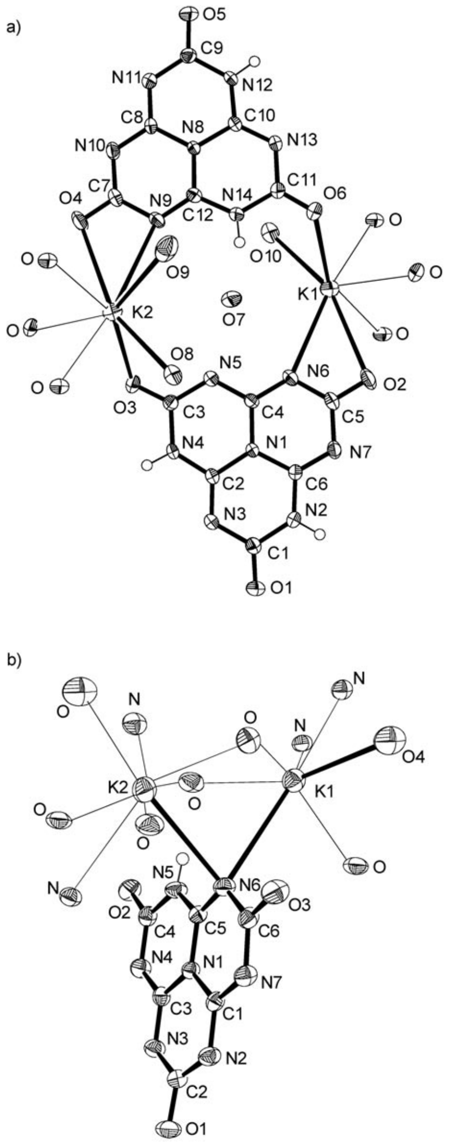

Figure 6. ORTEP diagrams of the asymmetric units of cyamelurate salts a) $K(C_6N_7O_3H_2)\cdot 2H_2O$ (**5**) and b) $K_2(C_6N_7O_3H)\cdot 1H_2O$ (**6**) (ellipsoids at 50% probability). Additional symmetry equivalent N and O atoms (labels without numbers) are shown to provide the full coordination geometry of the potassium ions. Hydrogen atoms of the crystal water molecules have been omitted for clarity.

Such a face-to-face stacking of flat aromatic molecules is typical and has been frequently observed. The distance between the anion layers of **5** and **6** is about 3.2 Å in both cases. Larger values for similar inter-layer distances of 3.6–3.7 Å were observed for alkali cyamelurates.[24] For potassium melonate $K_3[C_6N_7(NCN)_3]$[25] and melem[21] values around 3.3 Å were found, while this distance is 3.0–3.1 Å in melemium salts.[22] The potassium ions form a second type of layer, which contains water molecules in the case of **5**, while in the other salt **6** all the crystal water molecules are in the plane of the anions.

The coordination spheres of the cations (K1,K2) are relatively irregular. In **5**, for K1 six O atoms of the water mole-

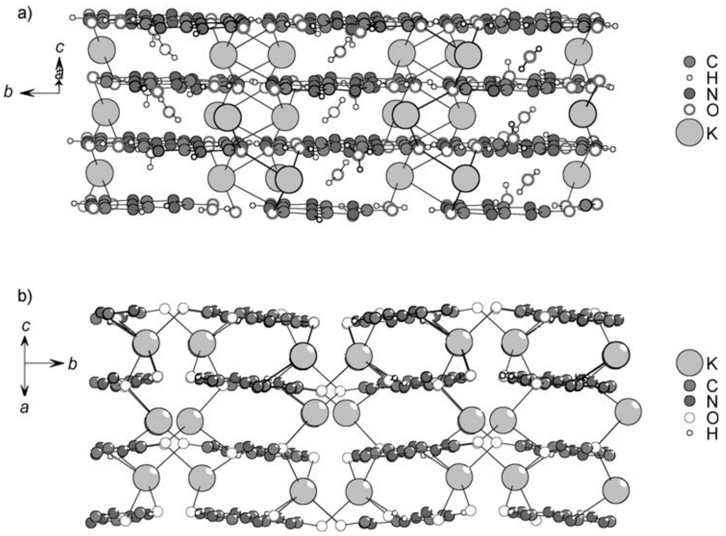

Figure 7. Cross sections of the crystal structures of a) $K(C_6N_7O_3H_2)\cdot 2H_2O$ (**5**) and b) $K_2(C_6N_7O_3H)\cdot 1H_2O$ (**6**) demonstrating the layered arrangement of the cyamelurate moieties.

cules and the anions as well as one N atom belong to the first coordination shell. K2 is coordinated by seven O atoms and one N atom (see Figure 6). In the coordination spheres of the cations (K1,K2) in **6**, both potassium atoms K1 and K2 are surrounded differently by five O atoms and three N atoms, sharing two oxygen atoms and one nitrogen ligand.

Very recently, a report on the crystal structure of the sodium dihydrogencyamelurate $Na[H_2(C_6N_7)O_3]\cdot 4H_2O$ was communicated.[50] Interestingly, this salt contains more water than the above discussed potassium salts. While the molecular structure of the anion is very similar to the above described structure of **5**, the coordination of the cations is much more symmetric, that is, nearly perfect NaO_6 octahedra are found without any metal–nitrogen coordination.

Crystal structures of 3b′ and 4: In order to provide clear evidence which isomeric forms are present in the case of compounds **3b′** and **4** we prepared single crystals suitable for X-ray structure analysis. Crystal parameters and refinement data are provided in Table 5, selected bond lengths and angles are summarized in Tables 8 and 9.

As depicted in Figure 8 there are six different tin atoms in the asymmetric unit of **3b′** coordinating to all six oxygen atoms of the cyameluric nucleus. Two of the four fivefold coordinated tin atoms, namely Sn1 and Sn2, form $OSn(Et_3)N$ trigonal bipyramidal double bridges between the two $C_6N_7O_3$ units. Sn4 and Sn5 form similar double bridges without Sn–N bonds, that is, $OSn(Et_3)O$ trigonal bipyramids. The Sn–O bond lengths vary between 2.23 and 2.40 Å and O/N–Sn–N bond angles are in the range between 167.3–171.6° indicating that the bipyramids are moderately distorted with all ethyl groups in equatorial positions. The C-Sn-C angles are in the range of 110.6–139.8°, deviating from the ideal value of 120°. The remaining two tin atoms Sn3 and Sn6 are tetrahedrally coordinated forming N-bonded triethylstannyl groups which are non-bridging. This results in a coordination polymer which may be derived from the tautomer **1-2-5** in Scheme 2. However, due to the fact that all three oxygen atoms form Sn–O bonds, the tautomers **1-2-6**, **1-2-8** and **1-3-6** may be considered as building blocks for the polymeric chains of **3b′** as well.

All Sn–C bond lengths vary only slightly between 2.12 and 2.16 Å independent of the tin atom and its coordination number. The Sn–N bonds, on the other hand, are 2.16 Å for the $NSnEt_3$ tetrahedra, but 2.50–2.53 Å for the trigonal bi-

Table 8. Selected bond lengths and bond angles of **3b′** (compare Figure 8).

Bond length [Å]		Bond angle [°]	
Sn1–O1	2.2287(16)	O1-Sn1-N12	167.33(6)
Sn1–N12	2.5262(17)	O1-Sn1-C(α)	89.17(8)–93.52(8)
Sn2–N2	2.4967(18)	N2-Sn2-O5	169.26(6)
Sn3–N5	2.1593(18)	N2-Sn2-C(α)	83.25(8)–100.26(13)
Sn4–O2	2.2708(17)	N5-Sn3-C(α)	100.87(9)–108.11(10)
Sn4–O4	2.3682(18)	O2-Sn4-O4	170.68(7)
Sn5–O3	2.4023(17)	O2/O4-Sn4-C(α)[i]	85.4(3)–97.72(9)
Sn5–O6	2.2693(16)	O3-Sn5-O6	171.63(6)
Sn6–N9	2.1607(19)	O3/O6-Sn5-C(α)[i]	85.28(8)–95.77(9)
$SnEt_3N/O–C$[a]	2.122(3)–2.161(3)	N9-Sn6-C(α)	103.19(9)–106.97(10)
$SnEt_3N–C$[b]	2.135(3)–2.160(3)	C(α)-Sn(L_5)-C′(α)[j]	110.62(16)–139.78(9)
O–C[c]	1.258(3)–1.266(3)	C(α)-Sn(L_4)-C′(α)[k]	107.1(4)–116.88(14)
C(O)–N(C,Sn)[d]	1.370(3)–1.388(3)	Sn-O-C (six angles)	114.34(14)–128.78(15)
C(O)–N(C)[e]	1.338(3)–1.374(3)	Sn(L_5)-N-C[l]	118.77(13)–123.43(14)
N(C_2)–C(N_3)[f]	1.304(3)–1.327(3)	Sn(L_4)-N-C[l]	112.75(13)–127.63(14)
C(N_3)–N(C,Sn)[g]	1.339(3)–1.353(3)	O-C-N (twelve angles)	115.79(19)–121.00(19)
C(N_3)–N(C_3)[h]	1.383(3)–1.407(3)	N-C(O)-N	122.2(2)–124.71(19)
		C(O)-N-C(N_3)[m]	116.98(16)–119.2(2)
		C(O)-N(Sn)-C(N_3)[n]	117.58(18)–119.22(18)
		N-C(N_3)-N(C_3)[o]	117.31(18)–122.33(18)
		C(N_3)-N(C_3)-C(N_3)′	118.40(17)–121.21(17)

[a] Range of all twelve different Sn–(α-C-ethyl) bond lengths of the five-fold coordinated tin atoms Sn1, Sn2, Sn4 and Sn5. [b] Six Sn–(α-C-ethyl) bond lengths of the four-fold coordinated tin atoms Sn3 and Sn6. [c] Six different C–O bond lengths. [d] Four different C(O)–N(Sn,C) bond lengths in the asymmetric unit. [e] Eight different C(O)–N(C) bond lengths. [f] Eight different bond lengths between non tin-coordinated N atoms and CN_3. [g] Four different bond lengths between tin-coordinated N atoms and CN_3. [h] Six different C–N bond lengths to the central N atoms. [i] Six different O–Sn–C bond angles on Sn4 and Sn5. [j] C-Sn-C′ angles for the fivefold coordinated tin atoms Sn1, Sn2, Sn4 and Sn5. [k] The C-Sn-C′ angles for the fourfold coordinated tin atoms Sn3 and Sn6. [l] Four different Sn-N-C angles on N2 and N12 as well as N5 and N9, respectively. [m] Eight different bond angles on the peripheral non tin-coordinated N atoms. [n] Four different bond angles on peripheral tin-coordinated N atoms. [o] Twelve different N–C–N bond angles involving the peripheral and the central N atoms.

Table 9. Selected interatomic distances and bond angles of **4** (compare Figure 9).

Bond length [Å]		Bond angle [°]	
Si–O[a]	1.7050(14)–1.7088(13)	C-Si-C[d]	110.64(14)–114.46(16)
Si–C[b]	1.826(3)–1.857(2)	C-Si-O[d]	100.36(10)–109.95(10)
C–O[a]	1.309(2)–1.3131(19)	Si-O-C[e]	126.43(12)–127.21(12)
C(O)–N[c]	1.332(2)–1.340(2)	O-C-N[f]	114.59(15)–117.27(15)
N(C$_2$)–C(N$_3$)[c]	1.323(2)–1.331(2)	N-C(O)-N[e]	127.94(15)–128.22(15)
C(N$_3$)–N7[a]	1.3994(19)–1.4048(19)	C(O)-N-C[f]	116.12(14)–116.90(15)
		N(C$_2$)-C-N(C$_3$)[f]	118.95(15)–121.25(15)
		C-N7-C[e]	119.92(12)–120.17(12)

[a] Range of three different bond lengths. [b] Nine different bond lengths. [c] Six different bond lengths. [d] Nine different bond angles. [e] Three different bond angles. [f] Six different bond angles.

pyramids. This observation may be attributed to the largely covalent Sn–C bond character compared with a significantly larger ionic contribution in the case of the Sn–N bonds.

A completely different situation is found for the silyl compound $C_6N_7O_3[Si(CH_3)_3]_3$ (**4**). The solvent free crystals contain isolated, π-stacked molecules. It is obvious from Figure 9 that the molecular structure is derived from the tautomeric form **1-4-7** of cyameluric acid (Scheme 2).

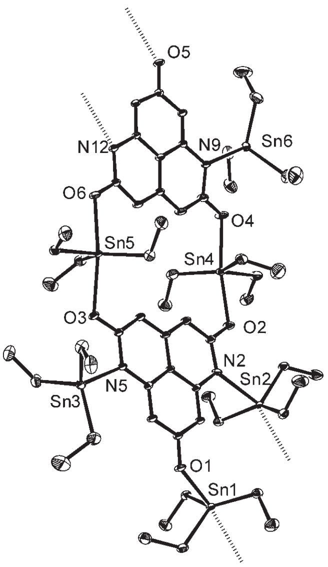

Figure 8. ORTEP diagram of $[C_6N_7O_3(SnEt_3)_3]_2{\cdot}C_2H_4Cl_2$ (**3b′**) (ellipsoids at 50% probability). Only a selection of the atoms has been labeled. All hydrogen atoms and the solvent molecules have been omitted for clarity (compare Table 8).

Similar to the above discussed salts **5** and **6** the 16-atom cyameluric $C_6N_7O_3$ unit is completely planar in both compounds **3b′** and **4**. The values for C–N bond lengths and N–C–N as well as C-N-C bond angles do not deviate significantly from the data found for other heptazine derivates (compare Table 1). That is to say, the central N atoms form the longest bonds to the surrounding carbon atoms with atom distances of 1.38–1.41 Å. Shorter are the C–N bonds between the C(N$_3$) atoms and the peripheral N(C$_2$) atoms. They are 1.32–1.33 Å in case of the silicon compound **4**. For compound **3b′** these C–N bonds are slightly elongated when the nitrogen atoms are coordinating to a tin atom, that is, 1.34–1.35 Å for C(N$_3$)–N(Sn,C$_2$) bonds versus 1.30–1.33 Å for C(N$_3$)–N(C$_2$). An analogous situation is observed for the remaining C–N bonds of the heptazine units: C(O)–N bonds are 1.34–1.37 Å while C(O)–N(Sn) bonds are 1.37–1.39 Å for **3b′**, and 1.33–1.34 Å for the silicon compound **4**. The C–O bond length in **4** of 1.31 Å is much closer to a C(sp^2)–O single bond than the C–O bond in **3b′** with an interatomic distance of 1.26–1.27 Å, which can be attributed to more ionic nature of the stannyl cyamelurate as compared to the silyl compound. Cyamelurates $M_3(C_6N_7O_3)$[24] as well as a cyameluric acid DMSO solvate are characterized by C–O distances of 1.26 Å.

With respect to bond angles, the deviations of formerly reported data for heptazine derivates are even smaller. The N-C(O)-N angles of the Si compound **4** are 128°, which is slightly increased when compared with the Sn compound **3b′** (122–125°). Values of 123–135° were reported for other heptazine compounds (see Table 1). All other angles within the $C_6N_7O_3$ units are in the range between 115 to 122°. Despite the differences in the C–O bond lengths mentioned

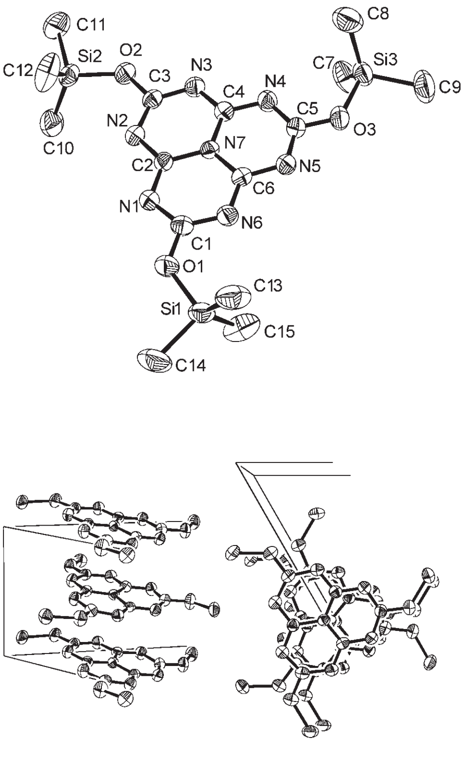

Figure 9. ORTEP diagrams of $C_6N_7O_3(SiMe_3)_3$ (**4**) (ellipsoids at 50% probability) showing the molecular structure and the arrangement of the molecules in the solid-state (compare Table 9). All hydrogen atoms have been omitted for clarity. Methyl groups have been omitted in the two packing diagrams.

above, the Sn-O-C and Si-O-C angles are also similar, that is, 114–129 for **3b′** and 126–127° for compound **4**, respectively. Interestingly, the Si atoms in **4** as well as the Sn atoms in **3b′** are located in the same plane as the $C_6N_7O_3$ units, as indicated by N-C-O-Si, O-C-N-Sn, N-C-N-Sn and N-C-O-Sn dihedral angles, respectively, which are all smaller than 15°.

The molecules in **4** are π-stacked along the *c* axis as shown in the lower part of Figure 9. The distance between the disc-like molecules of ~3.5 Å is close to the interlayer distance between similarly π-stacked cyamelurate anions in alkali cyamelurates, but bigger than the analogous distances in other neutral molecular heptazine compounds such as melem ($C_6N_7(NH_2)_3$),[21] triazido-tri-s-triazine ($C_6N_7(N_3)_3$),[8,23] or trichloro-tri-s-triazine ($C_6N_7Cl_3$)[4,26] (see above). Although the disc-like $C_6N_7O_3$-cyamelurate groups and all tin atoms of **3b′** also form layers, no π–π interaction is found in this structure. This is indicated by the relative large distance between these layers, which is around 6 Å. The ethyl groups and the non-coordinating 1,2-dichloroethane solvent molecules are located in the remaining space between the layers.

Thermal Stability of 3b, 4, 5 and 6: Recently, we reported on the thermal stability of alkali cyamelurates $M_3[C_6N_7O_3]$. The $C_6N_7O_3$ unit turned out to decompose at ~500 °C. This relatively high thermal stability was not found for the corresponding alkali cyanurates.[24] The TGA measurements of monopotassium cyamelurate and dipotassium cyamelurate show that these compounds are thermally stable up to temperatures around 400 °C. The decomposition temperatures of monopotassium cyamelurate (~400 °C) and dipotassium cyamelurate (~410 °C) are nearly identical. The TG curves of both salts show one step in the temperature range between 40 and 200 °C which is attributed to the loss of crystal water. The experimental value for the dehydration step in case of the monopotassium salt **5** was 12.0%, which is close to the calculated value of 12.2%, while this step in the case of the dipotassium salt can be attributed to a loss of 1.5 molecules of water (calcd value = 5.7% for $K_2(C_6N_7O_3H)\cdot 1\,H_2O$ (**6**), exptl value = 9.6%).

The DTA curves of compounds **5** and **6** show successive endothermic signals due to the evaporation of the crystal water, followed by decomposition of the cyameluric nucleus. The mass loss around 500–600 °C is not complete for both salts **5** and **6**. It is assumed that a potassium cyanate residue is formed, which decomposes under a nitrogen atmosphere above 750 °C.[51] This decomposition is accompanied by several exo- and endothermic signals in the DTA curves.

The thermal behavior of $C_6N_7O_3[Sn(C_2H_5)_3]_3\cdot C_2H_4Cl_2$ (**3b′**) and $C_6N_7O_3[Si(CH_3)_3]_3$ (**4**) is significantly different from the above discussed cyamelurate salts. The 1,2-dichloroethane solvent molecules of **3b′** evaporate even at ambient temperature. The TG (and DTG) curve of the solvent-free compound **3b** indicates that thermal decomposition starts at around 132 °C followed by a sharp step centered at 235 °C, which is due to a mass loss of 44%. This step is accompanied by an endothermic DTA signal. A second relatively sharp step of another 16% in the TG curve is located at 317 °C. A broader third step of 18% mass loss follows in the range between 360–480 °C. The latter two steps in the TG curve of **3b** are not characterized by any significant endo- or exothermic effects as shown by DTA. The final broad step between 540 and 690 °C on the other hand, is caused by exothermic reactions and results in another 15% mass loss. The residual 17% in mass does not change until the final measurement temperature of 1000 °C is reached.

In contrary to **3b** the Si compound **4** melts without any decomposition at around 200 °C, as indicated by a sharp endothermic DTA signal. A characteristic sharp mass loss of 74% is centered at 304 °C together with an endothermic effect. This may be correlated with a condensation reaction forming hexamethyl disiloxane $(CH_3)_3SiOSi(CH_3)_3$ and polymeric cyameluric acid anhydride $[C_6N_7O_{1.5}]_n$. Another clear endothermic event is observed at 480–530 °C, but without any decrease in mass. This temperature range is characteristic for the decomposition of the hepatzine C_6N_7 and/or the cyamelurate $C_6N_7O_3$ units, as was pointed out for the alkali cyamelurates and related compounds.[24,25] Finally, compound **4** decomposes completely into volatile species as indicated by as TG step at 652 °C and again an endothermic DTA signal.

In summary, both heptazine derivatives **3b** and **4** as well as the salts **5** and **6** decompose at lower temperatures as compared to the typical decomposition range found for the tricyclic C_6N_7 motive. In case of **5** and **6** this may be due to a deterioration of the conjugated π-system by protonation of the cyamelurate anions. In case of the silicon compound **4**, the decomposition is induced by the formation of the stable and volatile disiloxane, while **3b** thermally degrades at a relatively low temperature of 235 °C, presumably due the weak covalent bonds involving the tin atoms.

Conclusion

Analysis of the spectroscopic properties and in particular the single crystal X-ray structures of the metal organic compounds $C_6N_7O_3[Sn(C_2H_5)_3]_3\cdot C_2H_4Cl_2$ (**3b′**) and $C_6N_7O_3[Si(CH_3)_3]_3$ (**4**) as well as the mono- and dipotassium salts $K(C_6N_7O_3H_2)\cdot 2\,H_2O$ (**5**) and $K_2(C_6N_7O_3H)\cdot 1\,H_2O$ (**6**) reveal a detailed picture of the solid-state structures. Compounds **5** and **6** are examples for derivates of the carbonyl tautomers of cyameluric acid, while most other structurally characterized neutral and ionic species containing the cyameluric acid nucleus are derived from the trihydroxy tautomer **1-4-7** (Scheme 2).

As indicated by multi-nuclear solid-state NMR investigations and X-ray structures it is obvious that both salts, **5** and **6**, are derived from the tri-carbonyl tautomer **2-5-8** (Scheme 2). Therefore, it can be predicted that the most stable form of free cyameluric acid $C_6N_7O_3H_3$ has the same structure with C_{3h} symmetry. This conclusion is strongly supported by very recent structural examinations of a DMSO solvate[52] and a trihydrate[53] of cyameluric acid.

The thermal stability of **5** and **6** is decreased compared with alkali cyamelurates $M_3(C_6N_7O_3)$ as shown by decomposition temperatures of 400 versus 500 °C for the hydrogen free salts. The Si and Sn compounds $C_6N_7O_3[Sn(C_2H_5)_3]_3$ (**3b**) and $C_6N_7O_3[Si(CH_3)_3]_3$ (**4**) also decompose well below 500 °C.

Compound **4** can be considered as a tris-trimetylsilyl ester of **1-4-7**, containing fourfold coordinated silicon atoms. The tin compound **3b′**, on the other hand, contains two different bridging $OSnEt_3N$ as well as two different bridging $OSnEt_3O$ and terminal $NSiEt_3$ groups. The bridging tin atoms are characterized by a fivefold coordination forming trigonal bipyramids. The structural differences between **3b′** and **4** may simply be explained by the higher affinity of Si to oxygen compared with tin. Pearson's HSAB concept can also be used to explain the observed Sn–N coordination (soft–soft), which is not found for the silicon compound (hard–hard Si–O interactions).

Future experiments will show, if further derivatives of tautomers of cyameluric acid can be synthesized. It appears challenging to prepare representatives of all 17 tautomers (Scheme 2). Even more challenging is the idea to synthesize derivatives with *different* substituents in place of the three hydrogen atoms. Coming back to the graphitic carbon(IV) nitrides mentioned in the introduction, it remains an open question if and how the networks **II** and **IV** in Scheme 3 can be synthesized.

Experimental Section

General procedures, instruments and materials: All solvents and chemicals were used in p.a. quality as obtained from the suppliers. 1,1,1,3,3,3-Hexamethyldisilazane (HMDS) and 1,1,1,3,3,3-hexabutyldistannoxane were purchased from ABCR.

Tripotassium cyamelurate $K_3[C_6N_7O_3]$ and cyameluric acid $C_6N_7O_3H_3$ were synthesized according to the literature.[24] In brief, a suspension of melon powder (25 g) in a 2.5 molar aqueous KOH solution (250 mL) was heated under reflux for 45 min. The hot reaction mixture was filtered and slowly cooled to room temperature. Tripotassium cyamelurate was separated, washed with ethanol and dried at 100 °C under vacuum. The acid was obtained by precipitation with an excess of HCl (37 %). The white precipitate was immediately filtered off, washed with distilled water and dried at 100 °C under vacuum.

UV/Vis spectra were recorded with a Varian Cary 50 UV/Vis Spectrophotometer. The measurements were performed by taking samples during the pH-metric titration process.

FTIR spectra were obtained at room temperature using a Perkin Elmer 2000 FTIR spectrometer. The samples were thoroughly mixed with dry KBr. The preparation procedures were performed in a glovebox under dried argon atmosphere. The spectra were collected in a range from 400 to 4000 cm^{-1} with a resolution of 2 cm^{-1}.

TGA/DTA measurements were recorded using a STA 429 (Netzsch Gerätebau Gmbh). Under inert conditions 20 mg of the compound was filled into an alumina crucible and heated to 1000 °C (heating rate: 2 $K min^{-1}$) in a nitrogen atmosphere.

Solid-state ^1H, ^{13}C and ^{15}N MAS-NMR spectra were measured with a conventional impulse spectrometer DSX Avance (Bruker) operating with a resonance frequency of 400 MHz for ^1H ($B_0 = 9.4$ T). The samples were filled in zirconia rotors (diameter 4 mm) and mounted in a standard double-resonance MAS probe (Bruker). For all 1D MAS experiments the rotation frequencies ν_{rot} varied between 7 kHz and 12 kHz. ^1H and ^{13}C resonances are reported with respect to TMS and the ^{15}N signals are referenced using nitromethane. Integration and deconvolution of the MAS spectra were carried out with the commercial program package MATLAB.[54]

^1H MAS NMR data were acquired by exciting the FID with three back-to-back 90° pulses.[55] The sequence is designed to eliminate unwanted spectral contributions coming from the probe. The 90° pulse length was adjusted to 3 μs and the recycle delay varied between 20 and 80 s to guarantee total rebuild of magnetization due to spin-lattice relaxation. For the ^{13}C and ^{15}N MAS spectra ^1H–X cross-polarization double resonance experiments were performed with contact times t_H in the range of 10–40 ms. The long t_H ensure even the excitation of heteroatoms which are not covalently bonded to hydrogen. We employed a ramped cross-polarization sequence[56] by linearly reducing the ^1H radiation power from 100 % to 50 %. The FID was recorded using broadband proton decoupling with a TPPM sequence.[57] To enable a complete assignment of the ^{15}N resonances for compound **5** ($K(C_6N_7O_3H_2)\cdot 2H_2O$) additionally a cross-polarization polarization-inversion[21,58] (CPPI) filtered ^{15}N MAS spectrum was collected. The polarization inversion time t_i and ν_{rot} were set to 200 μs and 5 kHz, respectively.

Single crystal X-ray data were recorded on a Bruker-Nonius-X8 APEXII-CCD diffractometer (**3b′**, **4** and **5**) and on an Oxford Diffraction Excalibur-CCD diffractometer (**6**) with $Mo_{K\alpha}$ radiation. The structures were solved with direct methods, refined with full-matrix least-squares methods, all non-hydrogen atoms were anisotropically refined. Hydrogen atoms of **3b′** and **4** were placed in idealized positions and isotropically refined. The acidic hydrogen atoms (N-H and O-H) of **5** and **6** were detected by analysis of the residual electron density and isotropically refined. In case of **5** bond length restraints (SADI; same N−H and O−H bond lengths, respectively) were applied. Structure solution and refinement on F^2 against all reflections with the software SHELXS-97 and SHELXL-97 (G. M. Sheldrick, Universität Göttingen, **1986–1997**).

CCDC-600744 (**3b′**), -600743 (**4**), -600785 (**5**) and -602567 (**6**) contain the supplementary crystallographic data for this paper. These data can be obtained free of charge from The Cambridge Crystallographic Data Centre via www.ccdc.cam.ac.uk/data_request/cif

Titration experiment: Potassium cyamelurate $K_3[C_6N_7O_3]$ (110 mg, 0.32 mmol) was dissolved in de-ionized water (50 mL) and titrated against 0.1 M HCl. An automated pH titration system equipped with a Metrohm 713 pH meter was used. All measurements were performed at room temperature and after calibration of the glass-calomel electrode to ensure the accuracy of the pH values. At selected pH values the titration was interrupted in order to measure the UV/Vis spectra depicted in Figure 1.

Preparation of $K_2(C_6N_7O_3H)\cdot 1H_2O$ (6): Compound **6** was also synthesized by titration of a potassium cyamelurate $K_3[C_6N_7O_3]$ solution in de-ionized water against 0.1 M HCl. When a pH of 7.5 was reached a white precipitate had formed, which was separated by filtration. Single crystals of **6** were obtained from the filtrate by slow diffusion of ethanol vapor into the solution at room temperature. White crystals of $K_2(C_6N_7O_3H)\cdot 1H_2O$ were separated and dried in a desiccator over anhydrous calcium chloride. FTIR (see also Figure 2): $\tilde{\nu}$ = 3490(s), 2909(vw), 2830(vw), 2780(vw), 2752(vw), 1683(vs), 1476(vw), 1544(vs), 1476(m), 1450(m), 1402(vs), 1373(m), 1315 (m), 1183(w), 1141(m), 1116 (vw), 948(m), 888(w), 809(vs), 749(vw), 744(m), 662(vw), 647(vw), 616(vw), 541(vw), 465(s) cm^{-1}; elemental analysis calcd (%) for $K_2C_6N_7O_4H_3$ (315.35): C 22.85, H 0.96, N 31.09; found: C 22.99, H 1.14, N 30.76.

Preparation of $K(C_6N_7O_3H_2)\cdot 2H_2O$ (5): The above described titration was continued until a pH of 4.5 was reached. After separation of a precipitated solid by filtration white crystals of **5** were obtained by diffusion of ethanol into the solution via the vapor phase. The product was dried in a desiccator over anhydrous calcium chloride. FTIR (see also Figure 2): $\tilde{\nu}$ = 3415(s), 3069(br), 2790(vw), 2358(vw), 2041 (vw), 1685(vs), 1597(vw), 1583(vs), 1511(vs), 1474(vw), 1429(m), 1368(vs), 1301(s), 1172(w), 1141(w), 1071(vw), 1006(vw), 948(m), 796(vs), 778(vw), 692(vw), 680(w), 628(w), 605(w), 516(vw), 471(vw), 459(s) cm^{-1}; elemental analysis calcd (%) for $KC_6N_7O_5H_6$ (295.26): C 24.41, H 2.05, N 33.21; found: C 24.48, H 2.15, N 33.14.

Preparation of tris(trimethylsilyl)cyamelurate $C_6N_7(OSiMe_3)_3$ (4): Compound **4** was synthesized by heating cyameluric acid (2 g, 9 mmol) with 1,1,1,3,3,3-hexamethyldisilazane (HMDS) (3.55 g, 22 mmol) in the presence of $(NH_4)_2SO_4$ as a catalyst for 10 h at 160 °C under nitrogen, a white amorphous powder formed which was dried at 100 °C under vacuum. Yield: 3.84 g, 97 % (lit.:[45] 71.5 %); m.p. 179–198 °C (lit.:[45] 198–199 °C); FTIR (see also Figure 2): $\tilde{\nu}$ = 2963(w), 2903(vw), 1658vs), 1451(vs), 1294(w), 1256(vs), 1152(w), 1098(s), 1060(vw), 1011(m), 912(vw), 879(vs), 844(vs), 812 (w), 704(m), 636(m), 581(vw), 571(w), 447(w) cm^{-1}. Single crystals suitable for X-ray structure analysis were obtained by recrystallization from pentane.

Preparation of tris(tri-*n*-butylstannyl)cyamelurate $[C_6N_7O_3(Sn(nBu)_3)_3]$ (3a): Compound **3a** was synthesized by heating cyameluric acid (2.5 g, 11.3 mmol) with hexabutyldistannoxane (10.8 g, 18.14 mmol) for 6 h at 150 °C under nitrogen. A white amorphous powder is separated and dried at 100 °C under vacuum. Yield: 11.7 g, 95 % (lit.:[45] 97.5 %); softening point = 102 °C (lit.: [45] > 105 °C); FTIR (see also Figure 2): $\tilde{\nu}$ = 2957(vs), 2900(vs), 2846(vw), 2853(s), 1666(vw), 1654(s), 1606(w), 1522(vs), 1526(vs), 1458(w), 1427(vw), 1398(s), 1375(vw), 1297(vw), 1292(w), 1195(vw), 1146(w), 1195(w), 1146(vw), 1073(m), 838(vw), 959(vw), 928(vw), 876(m), 811(m), 771(vw), 670(m), 599(m), 517(w), 454(vw), 449(m) cm^{-1}; elemental analysis calcd (%) for $C_{42}H_{81}N_2O_3Sn$ (780.83): C 46.36, H 7.50, N 9.01; found: C 46.30, H 7.98, N 9.28.

Preparation of tris(triethylstannyl)cyamelurate $[C_6N_7O_3(SnEt_3)_3]$ (3b): Compound **3b** was synthesized by heating cyameluric acid (1.034 g, 4.67 mmol) with hexaethyldistannoxane (2.99 g, 7.02 mmol) for 20 h at 130 °C under nitrogen in the presence of dry toluene as a solvent. A white amorphous powder had formed, which was separated and dried at 100 °C under vacuum. Yield: 3.70 g, 95 %; m.p. 280 °C(decomp); FTIR: $\tilde{\nu}$ = 3482(vw), 3329(m), 3118(vw), 3059(vw), 2949(s), 2868(s), 2770(w), 2726(vw), 2347(vw), 2339(vw), 2265(vw), 2133(vw), 2059(vw), 1685(s), 1652(s), 1605(vw), 1584(vw), 1540(vs), 1479(s), 1451(s), 1403(vs), 1369(w), 1314(m), 1260(w), 1192(w), 1141(m), 1141(w), 1080(w), 1016(m), 957(m), 885(vw), 824(vw), 806(vs), 773(vw), 747(w), 675(s), 647(vw), 600(vw), 518(s), 464(s), 421(vw), 394(w) cm^{-1}; elemental analysis calcd (%) for $C_{24}H_{45}N_7O_3Sn_3$ (835.80): C 34.49, H 5.49, N 11.73; found: C 33.50, H 5.16, N 12.97. Single crystals of the solvate $[C_6N_7O_3(SnEt_3)_3]_2 \cdot C_2H_4Cl_2$ (**3b′**) suitable for X-ray structure analysis were obtained by recrystallization from dichloroethane.

Acknowledgements

We gratefully acknowledge the German Research Foundation (DFG project KR 1739/9-1 and project SE 1417/1-1) and the Alexander von Humboldt foundation (postdoctoral fellowship for N.E.A. E.-G.) for financial support; Dominik Wöll for performing the titration and UV absorption measurements; Stephan Siroky for performing the simultaneous thermal analysis (STA); and Tobias Gmeiner, Vadym Bakumov and John Barber for helpful input. Uwe Böhme is acknowledged for the calculating structural and electronic properties of cyameluric acid derivates and FTIR as well as UV spectra simulation and interpretation. We thank Professor E. Rößler for the opportunity to carry out the measurements at the solid-state NMR spectrometer in his laboratory.

---

[1] Further synonyms: *sym*-heptazine, 1,3,4,6,7,9,9b-heptaaza-phenallene, 1,3,4,6,7,9-heexaazacyclo[3.3.3]azine or cyamelurine.

[2] M. Cyranski, T. M. Krygowski, *Tetrahedron* **1996**, *52*, 13795–13802.

[3] See for example: G. Giacomelli, A. Porcheddu, L. de Luca, *Curr. Org. Chem.* **2004**, *8*, 1497–1519.

[4] E. Kroke, M. Schwarz, E. Horvath-Bordon, P. Kroll, B. Noll, A. D. Norman, *New J. Chem.* **2002**, *26*, 508–512.

[5] Review: E. Kroke, M. Schwarz, *Coord. Chem. Rev.* **2004**, *248*, 493–532.

[6] a) M. L. Cohen, *Phys. Rev. B* **1985**, *32*, 7988–7991; b) A. Y. Liu, M. L. Cohen, *Science* **1989**, *245*, 841–842; c) A. Y. Liu, M. L. Cohen, *Phys. Rev. B* **1990**, *41*, 10727–10734.

[7] a) J. Liebig, *Ann. Chem.* **1834**, *10*, 10; b) W. Henneberg, *Ann. Chem.* **1850**, *73*, 228; c) J. Liebig, *Ann. Chem.* **1850**, *10*, 257–282.

[8] E. Kroke, Habilitation, TENEA, Berlin, **2004**, pp. 183–202 (in German).

[9] L. Pauling, J. H. Sturdivant, *Proc. Natl. Acad. Sci. USA* **1937**, *23*, 615–620.

[10] a) C. E. Redemann, H. J. Lucas, *J. Am. Chem. Soc.* **1939**, *61*, 3420–3425; b) C. E. Redemann, H. J. Lucas, *J. Am. Chem. Soc.* **1940**, *62*, 842–846.

[11] a) A. I. Finkel'shtein, *Zh. Obshch. Khim.* **1961**, *31*, 1132–1135; b) A. I. Finkel'shtein, N. V. Spiridonova, *Zh. Org. Khim.* **1964**, *1*, 606–609; c) A. I. Finkel'shtein, N. V. Spiridonova, *Russ. Chem. Rev.* **1964**, *33*, 400–405; d) A. G. Koryakin, V.A. Gal′perin, A. N. Sarbaev, A. I. Finkel'shtein, *Zh. Org. Khim.* **1971**, *7*, 972–977; e) N. I. Zhagrova, N. V. Spiridonova, A. I. Finkel'shtein, *Zh. Prikl. Spektrosk.* **1973**, *19*, 153–154; f) N. I. Zhagrova, N. V. Spiridonova, A. I. Finkel'shtein, *Zh. Prikl. Khim.* **1975**, *48*, 452–453.

[12] a) R. S. Hosmane, M.A. Rossman, N. J. Leonard, *J. Am. Chem. Soc.* **1982**, *104*, 5497–5499; b) M. Shahbaz, S. Urano, P. R. LeBreton, M.A. Rossman, R. S. Hosmane, N. J. Leonard, *J. Am. Chem. Soc.* **1984**, *106*, 2805–2811; c) A. M. Halpern, M.A. Rossman, R. S. Hosmane, N. J. Leonard, *J. Phys. Chem.* **1984**, *88*, 4324–4326; d) M.A. Rossmann, N. J. Leonard, S. Urano, P. R. LeBreton, *J. Am. Chem. Soc.* **1985**, *107*, 3884–3890.

[13] See for example: Y. Morita, T. Aoki, K. Fukui, S. Nakazawa, K. Tamaki, S. Suzuki, A. Fuyuhiro, K. Yamamoto, K. Sato, D. Shiomi, A. Naito, T. Takui, K. Nakasuji, *Angew. Chem.* **2002**, *114*, 1871–1874; *Angew. Chem. Int. Ed.* **2002**, *41*, 1792–1796.

[14] See for example: S. Suzuki, Y. Morita, K. Fukui, K. Sato, D. Shiomi, T. Takui, K. Nakasuji, *Inorg. Chem.* **2005**, *44*, 8197–8199.

[15] See for example: M. Fourmigue, H. Eggert, K. Bechgaard, *J. Org. Chem.* **1991**, *56*, 4858–4864.

[16] See for example: a) F. Tran, B. Alameddine, T. A. Jenny, T. A. Wesolowski, *J. Phys. Chem. A* **2004**, *108*, 9155–9160; b) J. E. Field, D. Venkataraman, *Chem. Mater.* **2002**, *14*, 962–964.

[17] See for example: A. C. M. Carvalho, M. C. Dos Santos, *J. Non-Cryst. Solids* **2004**, *338–340*, 254–257.

[18] See for example: a) S. Souto, M. Pickholz, M. C. dos Santos, F. Alvarez, *Phys. Rev. B* **1998**, 57, 2536–2540.

[19] See for example: M. Vaziri, *Mater. Lett.* **2006**, 60, 926–928.

[20] See for example: C. P. Ewels, M. Glerup, *J. Nanosci. Nanotechnol.* **2005**, 5, 1345–1363.

[21] a) B. Jürgens, E. Irran, J. Senker, P. Kroll, H. Müller, W. Schnick, *J. Am. Chem. Soc.* **2003**, *125*, 10288–10300; b) A. Sattler, W. Schnick, *Z. Anorg. Allg. Chem.* **2006**, *632*, 238–242.

[22] A. Sattler, L. Seyfarth, J. Senker, W. Schnick, *Z. Anorg. Allg. Chem.* **2005**, *631*, 2545–2554.

[23] D. R. Miller, D. C. Swenson, E. G. Gillan, *J. Am. Chem. Soc.* **2004**, *126*, 5372–5373.

[24] E. Horvath-Bordon, E. Kroke, I. Svoboda, H. Fueß, R. Riedel, N. Sharma, A.K. Cheetham, *Dalton Trans.* **2004**, 3900–3908.

[25] E. Horvath-Bordan, E. Kroke, I. Svoboda, H. Fueß, R. Riedel, *New J. Chem.* **2005**, *29*, 693–699.

[26] S. Tragl, H.-J. Meyer, *Z. Anorg. Allg. Chem.* **2005**, *631*, 2300–2302.

[27] B. Traber, T. Oeser, R. Gleiter, M. Goebel, R. Wortmann, *Eur. J. Org. Chem.* **2004**, 4387–4390.

[28] G. K. Williams, S. F. Palopoli, T. B. Brill, *Combust. Flame* **1994**, 98, 197–204.

[29] Heptazine derivatives are mentioned in almost any patent application related to flame retardants, for recent examples see: a) C. Perego, F. P. M. Mercx, R. Puyenbroek, R. Kumaraswamy, H. Manjunath, S. Charati (General Electric Company, USA), PCT Int. Appl., WO 2005118698 A1, **2005**; b) G. I. Titelman, S. Bron, (Bromine Compounds Ltd., Israel), PCT Int. Appl., WO 2005101976 A2, **2005**; c) X. Couillens, M. Amorese (Rhodia Engineering Plastics S.R.L., Italy), PCT Int. Appl., WO 2005061606 A1, **2005**; d) H.

Ohyama, H. Matsui, N. Maeda (Mitsubishi Engineering-Plastics Corporation, Japan), Eur. Pat. Appl., EP 1533343 A1, **2005**.

[30] W. Zheng, N.-B. Wong, G. Zhou, X. Liang, J. Li, A. Tian, *New J. Chem.* **2004**, *28*, 275–283.

[31] a) S. Ono, T. Funato, Y. Inoue, T. Munechika, T. Yoshimura, H. Morita, S.-I. Rengakuji, C. Shimasaki, *J. Chromatogr.* **1998**, *815*, 197–204; b) S. Ono, Y. Inoue, N. Watanabe, T. Yoshimura, H. Morita, A. Shiroishi, M. Takakura, C. Shimasaki, *J. Chromatogr.* **1996**, *752*, 287–290.

[32] a) T. B. Gavrilova, Y. S. Nikitin, T. A. Rudnitskaya, *Zh. Fiz. Khim.* **1994**, *68*, 545–550; b) T. B. Gavrilova, Y. S. Nikitin, T. A. Rudnitskaya, A. I. Finkel'shtein, *Zh. Fiz. Khim.* **1992**, *66*, 1080–1084.

[33] a) W. Zheng, N.-B. Wong, W. Wang, G. Zhou, A. Tian, *J. Phys. Chem. A* **2004**, *108*, 97–106; b) W. Zheng, N.-B. Wong, X. Liang, X. Long, A. Tian, *J. Phys. Chem. A* **2004**, *108*, 840–847; c) X. Liang, W. Zheng, N.-B. Wong, J. Li, A. Tian, *THEOCHEM* **2004**, *672*, 151–159; d) W. Zheng, N.-B. Wong, W.-K. Li, A. Tian, *J. Phys. Chem. A* **2004**, *108*, 11721–11727; e) W. Zheng, N.-B. Wong, A. Tian, *J. Phys. Chem. A* **2005**, *109*, 1926–1932.

[34] I. Alkorta, N. Jagerovic, J. Elguero, *ARKIVOC* **2004**, *4*, 130–136.

[35] C. Zhang, Y. Shu, X. Wang, X. Zhao, B. Tan, R. Peng, *J. Phys. Chem. A* **2005**, *109*, 6592–6596.

[36] P. G. Karamertzanis, C. C. Pantelides, *J. Computational Chem.* **2005**, *26*, 304–324.

[37] E. M. Smolin, L. Rapoport, "s-Triazines and derivatives" in *The chemistry of heterocyclic compounds*, *Vol. 13* (Ed.: A. Weissberger), Interscience, New York, **1959**.

[38] P. Gamez, J. Reedijk, *Eur. J. Inorg. Chem.* **2006**, 29–42.

[39] a) A. Hofmann, *Chem. Ber.* **1886**, *19*, 2061; b) M. L. Tosato, L. Soccorsi, *J. Chem. Soc. Perkin Trans. 2* **1982**, 1321–1326.

[40] P. J. Harrington, I. H. Sanchez, *Synth. Commun.* **1993**, *23*, 1307–1314.

[41] a) I. Alves, G. Demazeau, B. Tanguy, F. Weill, *Solid State Commun.* **1999**, *109*, 697–701; b) M. Mattesini, S. F. Matar, J. Etourneau, *J. Mater. Chem.* **2000**, *10*, 709–713.

[42] See for example: E. K. Wilson, *Chem. Eng. News*, May 31, **2004**, 34–36.

[43] M. Takimoto, *Nippon Kagaku Zasshi* **1964**, *85*, 159–168 (in Japanese).

[44] G. Huyge-Tiprez, J. Nicole, *Comptes Rendus des Seances de l'Academie des Sciences, Serie C: Sciences Chimiques* **1977**, 284, 913–915 (in French).

[45] Y. I. Dergunov, A. S. Gordetsov, I. A. Vostokov, E. N. Boitsov, *Zh. Obshch. Khim.* **1976**, *46*, 1653–1654.

[46] A. S. Gordetsov, A. P. Kozina, S. E. Skobeleva, Y. I. Mushkin, R. P. Zakharova, Y. I. Dergunov, *Metalloorg. Khim.* **1989**, *2*, 1129–1135.

[47] X. J. Ai, F. Deng, J. X. Dong, W. Hu, H. Xu, C. H. Ye, *Solid State Nucl. Magn. Reson.* **2004**, *25*, 216–226.

[48] C. Gardiennet, P. Tekely, *J. Phys. Chem. B* **2002**, *106*, 8928–8936.

[49] X. Xue, M. Kanzaki, *J. Phys. Chem. B* **2001**, *105*, 3422–3434.

[50] A. Sattler, W. Schnick, *Z. Anorg. Allg. Chem.* **2006**, *632*, 531–533.

[51] G. B. Seifer, D. A. Prokoshkin, *Dokl. Akad. Nauk SSSR* **1979**, *245*, 162–166.

[52] J. Wagler, N. E. A. El-Gamel, E. Kroke, *Z. Naturforsch. B*, **2006**, 69, 975–978.

[53] A. Sattler, W. Schnick, *Z. Anorg. Allg. Chem.*, **2006**, *632*, 1518–1523.

[54] MATLAB, The Language of Technical Computing, MathWorks Inc., Copyricht 1984–1998, 24 Prime Park Way, Natick, MA 01760-1500.

[55] S. Zhang, X. Wu, M. Mehring, *Chem. Phys. Lett.* **1990**, *173*, 481–484.

[56] a) S. C. Shekar, A. Ramamoorthy, *Chem. Phys. Lett.* **2001**, *342*, 127–134; b) G. Metz, X. L. Wu, S. O. Smith, *J. Magn. Reson. A110*, 219–227.

[57] A. E. Bennett, C. M. Rienstra, M. Auger, K. V. Lakshmi, R. G. Griffin, *J. Chem. Phys.* **1995**, *103*, 6951–6958.

[58] X. Wu, K. W. Zilm, *J. Magn. Reson.* **1993**, *A102*, 205–213.

Received: March 30, 2006